

A Preconditioned Difference of Convex Algorithm for Truncated Quadratic Regularization with Application to Imaging

Shengxiang Deng · Hongpeng Sun

Received: date / Accepted: date

Abstract We consider the minimization problem with the truncated quadratic regularization, which is a nonsmooth and nonconvex problem. We cooperated the classical preconditioned iterations for linear equations into the nonlinear difference of convex functions algorithms with extrapolation. Especially, our preconditioned framework can deal with the large linear system efficiently which is usually expensive for computations. Global convergence is guaranteed and local linear convergence rate is given based on the analysis of the Kurdyka-Lojasiewicz exponent of the minimization functional. The proposed algorithm with preconditioners turns out to be very efficient for image restoration and is also appealing for image segmentation.

Keywords nonconvex optimization · image restoration · difference of convex functions algorithm (DCA) · linear preconditioning techniques · Kurdyka-Lojasiewicz analysis

Mathematics Subject Classification (2010) 65K10 · 49J52 · 49M15

1 Introduction

In this paper, we consider the truncated quadratic regularization with gradient operator for image restoration and segmentation

$$\arg \min_{\mathbf{x} \in X} F(\mathbf{x}) = f(\mathbf{x}) + P^I(\mathbf{x}), \quad P^I(\mathbf{x}) := \sum_{i=1}^m \sum_{j=1}^n \frac{\mu}{2} \min(|(\nabla \mathbf{x})_{i,j}|^2, \frac{\lambda}{\mu}), \quad (\text{ITQ})$$

$$\arg \min_{\mathbf{x} \in X} F(\mathbf{x}) = f(\mathbf{x}) + P^A(\mathbf{x}), \quad P^A(\mathbf{x}) := \sum_{i=1}^m \sum_{j=1}^n \frac{\mu}{2} \sum_{l=1}^2 \min(|(\nabla_l \mathbf{x})_{i,j}|^2, \frac{\lambda}{\mu}), \quad (\text{ATQ})$$

Shengxiang Deng
Institute for Mathematical Sciences, Renmin University of China, Beijing, China.
E-mail: 2018103581@ruc.edu.cn

Hongpeng Sun
Institute for Mathematical Sciences, Renmin University of China, Beijing, China.
E-mail: hpsun@amss.ac.cn

where λ and μ are positive constants, $X := \mathbb{R}^{m \times n}$ is a finite dimensional discrete image space, $\nabla = [\nabla_1, \nabla_2]^T$ and $f(\mathbf{x}) := \|\mathbf{A}\mathbf{x} - \mathbf{x}_0\|_2^2/2$ with $\mathbf{A} : X \rightarrow Y_0 = \mathbb{R}^{m_0 \times n_0}$ being a linear and bounded operator and \mathbf{x}_0 being the noisy or degraded image. Here and subsequently, the $|\cdot|$ norm denotes the usual Euclid norm which is also the length of the corresponding vector. For example, $|(\nabla \mathbf{x})_{i,j}| = \sqrt{(\nabla_1 \mathbf{x})_{i,j}^2 + (\nabla_2 \mathbf{x})_{i,j}^2}$ for the isotropic case in (ITQ) and $|(\nabla_l \mathbf{x})_{i,j}|$ is the absolute value of $(\nabla_l \mathbf{x})_{i,j}$ with $l = 1$ or $l = 2$ in (ATQ). P^I or P^A is the isotropic or anisotropic truncated quadratic regularizations (abbreviated as ITQ or ATQ). The truncated quadratic (also called as half-quadratic) regularization has various applications in signal, image processing and computer vision [4, 5, 10, 11, 20, 38]. It was originated from the maximal posterior estimates for the Markov random fields within the probabilistic setting mainly the Bayesian framework [18]. It also appeared as the weak membrane energy and the corresponding graduated non-convexity algorithm developed in [11]. The nonsmooth and nonconvex truncated quadratic regularization without gradient operator was also found in robust statistic where it can kill the outliers completely [19, 40]; see Figure 1 for the absolute value function and the truncated quadratic function. The discrete truncated quadratic regularization can also be seen as the discrete version of the continuous variational Mumford-Shah functional [14, 30, 31, 40]. We refer to [42] for the general framework of truncated regularization which covered the truncated quadratic problem. Due to so many important applications in imaging and other fields, there are already a lot of studies on algorithmic developments for this problems [20, 33]. Generally, there are two categories of algorithms. One is the stochastic approximation approach including the simulated annealing and the other is the deterministic approach. There are many kinds of deterministic optimization algorithms including the graph-cut algorithm [10] and the graduated non-convexity algorithm (GNC) [11]; see [13, 32] for its recent development. Fast algorithms are also developed in [4, 5, 15, 16] which benefit from the alternating minimization technique by introducing some auxiliary variables [20, 29].

Inspired by the recent developments of the difference of convex algorithms (DCA) [21–23, 41] and the powerful Kurdyka-Lojasiewicz (KL) analysis for nonconvex optimizations [1–3, 24, 39] together with the preconditioned techniques in convex splitting algorithms [6–8], we tackle this problem by the proposed preconditioned DCA algorithm with extrapolation. DCA is now widely used for analyzing and computing nonconvex models in image and signal processing. For example, a weighted difference of anisotropic and isotropic TV model is proposed in [26] for better reconstruction and a more delicate l_1 - αl_2 model is further developed in [25]. For (ITQ) or (ATQ), we will employ the following difference of convex functions (DC) throughout this paper, $P^l(\mathbf{x}) = P_1^l(\mathbf{x}) - P_2^l(\mathbf{x})$ with $l = I$ or $l = A$ and

$$\begin{aligned} P_1^I(\mathbf{x}) &= \sum_{i=1}^m \sum_{j=1}^n \frac{\mu}{2} (|(\nabla \mathbf{x})_{i,j}|^2 + \frac{\lambda}{\mu}), & P_2^I(\mathbf{x}) &= \sum_{i=1}^m \sum_{j=1}^n \frac{\mu}{2} \max(|(\nabla \mathbf{x})_{i,j}|^2, \frac{\lambda}{\mu}), \\ P_1^A(\mathbf{x}) &= \sum_{i=1}^m \sum_{j=1}^n \frac{\mu}{2} \sum_{l=1}^2 (|(\nabla_l \mathbf{x})_{i,j}|^2 + \frac{\lambda}{\mu}), & P_2^A(\mathbf{x}) &= \sum_{i=1}^m \sum_{j=1}^n \frac{\mu}{2} \sum_{l=1}^2 \max(|(\nabla_l \mathbf{x})_{i,j}|^2, \frac{\lambda}{\mu}). \end{aligned} \quad (1.1)$$

Note that both $f(\mathbf{x})$, $P_1^I(\mathbf{x})$ and $P_2^I(\mathbf{x})$ (or $P_1^A(\mathbf{x})$ and $P_2^A(\mathbf{x})$) are convex functions. P_1^I (or P_1^A) is continuous differentiable with locally Lipschitz gradient and P_2^I (or P_2^A) is proper closed function. Our motivation mainly comes from the challenging problem for solving the linear subproblems appeared in DCA, which is the most expensive step for DCA in a lot of applications [21]. For example, splitting decomposition algorithm with error control is employed in [21]. We proposed a preconditioned framework and cooperated the preconditioned iteration for linear systems into the

total nonlinear DCA iterations. In this framework, only one or few preconditioned steps are needed for the linear subproblems without solving it inexactly or exactly. Especially, the global convergence and the local linear convergent rate of DCA can also be obtained. Usually, the computational amount of one time or few times preconditioned iterations is quite less. For example, the computation effort of one Jacobi or one symmetric Gauss-Seidel iteration for large scale linear system is nearly negligible compared to solving the linear sytem even with moderate accuracy, especially for large scale linear system.

Our contributions belong to the following parts. First, we propose a preconditioned DCA for the truncated quadratic regularization with gradient operator including both the isotropic and anisotropic cases. With the classical preconditioning technique, we can deal with the large linear system efficiently for the nonlinear DCA algorithm with any finite time preconditioned iterations. No error control is needed for solving large linear systems while the convergence can be guaranteed. For example, in the proposed preconditioned framework, one can still obtain global convergence of the DCA by employing 10 specially designed symmetric red-black Gauss-Seidel iterations for the linear subproblem during each DCA iteration. Second, with detailed analysis of the Kurdyka-Lojasiewicz exponent of the minimization functional, together with the global convergence of the iterative sequence, we also prove the local linear convergence rate of the proposed preconditioned DCA. Third, our global convergence and local convergence rate analysis is based on the difference of convex structure (1.1) where P_1 (P_1^I or P_1^A) has locally Lipschitz gradient and P_2 (P_2^I or P_2^I) is closed and convex. This is different from the case in [39] where P_1 is closed and convex and P_2 has locally Lipschitz gradient. Fourth, we also explore the feature of the truncated quadratic regularization for image segmentation within the proposed preconditioned DCA framework, which was already studied by a lot of algorithms including the graduated non-convexity algorithm [11], the graph-cut based discrete optimization method [10], and the primal-dual first-order method [38]. Besides the image segmentation, it is known that the truncated quadratic regularization can also be used for image denoising. However, there is no systematic comparisons with the total variation regularization. We give some comparisons between the truncated quadratic regularization and the total variation for image denoising with detailed parameters.

The rest of the paper is organized as follows. In section 2, after some preparations and the calculation of the Kurdyka-Lojasiewicz exponent, we give the global convergence and present the local linear convergence rate of the proposed preconditioned and extrapolated DCA. In section 3, we give a systematic numerical study on the image denoising and image segmentation. Finally, we give some discussions on section 4.

2 Preconditioned DCA_e: convergence and preconditioners

2.1 Preliminaries and KL exponent analysis

Let $h : \mathbb{R}^n \rightarrow \mathbb{R} \cup \{+\infty\}$ be a proper lower semicontinuous function. Denote $\text{dom } h := \{x \in \mathbb{R}^n : h(x) < +\infty\}$. For each $x \in \text{dom } h$, the limiting-subdifferential of h at $x \in \mathbb{R}^n$, written ∂h , is defined as follows [28, 35],

$$\partial h(x) := \left\{ \xi \in \mathbb{R}^n : \exists x_n \rightarrow x, h(x_n) \rightarrow h(x), \xi_n \rightarrow \xi, \liminf_{y \rightarrow x, y \neq x_n} \frac{h(y) - h(x_n) - \langle \xi_n, y - x_n \rangle}{|y - x_n|} \geq 0 \right\}.$$

It is known that the above subdifferential ∂h reduces to the classical subdifferential in convex analysis when h is convex. It can be seen that a necessary condition for $x \in \mathbb{R}^n$ to be a minimizer of h

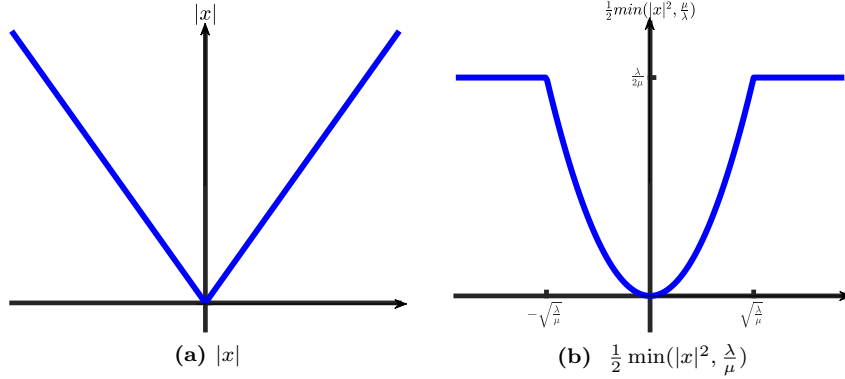


Fig. 1: Absolute value function and truncated quadratic function in \mathbb{R} .

is $0 \in \partial h(x)$ [1]. For the global and local convergence analysis, we also need the Kurdyka-Lojasiewicz (KL) property and KL exponent.

Definition 1 (KL property and KL exponent) A proper closed function h is said to satisfy the KL property at $\bar{x} \in \text{dom } \partial h$ if there exists $a \in (0, +\infty]$, a neighborhood \mathcal{O} of \bar{x} , and a continuous concave function $\psi : [0, a) \rightarrow (0, +\infty)$ with $\psi(0) = 0$ such that:

- (i) ψ is continuous differentiable on $(0, a)$ with $\psi' > 0$.
- (ii) For any $x \in \mathcal{O}$ with $h(\bar{x}) < h(x) < h(\bar{x}) + a$, one has

$$\psi'(h(x) - h(\bar{x})) \text{dist}(0, \partial h(x)) \geq 1. \quad (2.1)$$

A proper closed function h satisfying the KL property at all points in $\text{dom } \partial h$ is called a KL function. If ψ in (2.1) can be chosen as $\psi(s) = cs^{1-\theta}$ for some $\theta \in [0, 1)$ and $c > 0$, we say that h satisfies KL properties at \bar{x} with exponent θ . This means that for some $\bar{c} > 0$, we have

$$\text{dist}(0, \partial h(x)) \geq \bar{c}(h(x) - h(\bar{x}))^\theta. \quad (2.2)$$

If h satisfies KL property with exponent $\theta \in [0, 1)$ at all the points of $\text{dom } \partial h$, we call h is a KL function with exponent θ .

The following *uniformized KL property* proved in [9] is also important for our discussions.

Lemma 1 Assume h is a proper closed function and Γ is a compact set. If h is a constant on Γ and satisfies the KL property at each point of Γ , then there exist $\epsilon, a > 0$ for any ψ as in definition 1,

$$\psi'(h(x) - h(\hat{x})) \text{dist}(0, \partial h(x)) \geq 1, \quad (2.3)$$

for any $\hat{x} \in \Gamma$ and any x satisfying $\text{dist}(x, \Gamma) < \epsilon$ and $h(\hat{x}) < h(x) < h(\hat{x}) + a$.

The minimization problem (ITQ) or (ATQ) is a standard DC programming and can be solved by DCA. From now on, we will denote x as the vectorized \mathbf{x} . We will still use the same notations A, Δ, A^* and ∇ (or F, f and P) as the matrix version of the linear mappings (the functions) after

vectorization. Let's take the problem (ITQ) for example. The standard DCA iteration reads as follows,

$$x^{t+1} := \arg \min_x f(x) + P_1^I(x) - \langle \xi^t, x \rangle, \quad \xi^t \in \partial P_2^I(x)|_{x=x^t}, \quad (2.4)$$

where P_1^I , f and P_2^I are the same functions in (1.1) and the term $\langle \xi^t, x \rangle$ essentially represents the linearization of the convex function $P_1^I(x)$ through its subgradient. It can be seen by replacing $\langle \xi^t, x \rangle$ by $\langle \xi^t, x - x^t \rangle + P_2^I(x^t)$ in (2.4) without changing the minimization problem (2.4). By direct calculation, the minimizer x^{k+1} of (2.4) can be obtained by solving the following linear equation during each DCA iteration

$$(A^*A - \mu\Delta)x = \xi^t + A^*x_0. \quad (2.5)$$

It is very expensive and challenging to solve this kind of equation especially for large linear systems during each iteration even with error control. In [21], ‘‘preconditioned decomposition algorithm’’ is employed to solve the equation with error control while A is the identity operator in (2.5). Inspired by the preconditioned framework for the convex splitting algorithm [6–8], our motivation is to introduce the powerful and classical preconditioning technique for linear systems such as (2.5) and cooperate them into the nonlinear DCA.

We introduce the preconditioned iterations for (2.5) through proximal terms with special metric (or weight). Let's first introduce the inner product and norm induced by the positive definite and self-adjoint operator (metric) M ,

$$\langle x, y \rangle_M := \langle x, My \rangle, \quad \|x\|_M^2 := \langle x, Mx \rangle.$$

Moreover, we will also employ the extrapolation framework that can bring out certain acceleration [39] for a lot of cases. The extrapolation strategy is originated from Nesterov's accelerated gradient method. To this end, let's introduce the extrapolation parameter β such that $\{\beta_t\} \subseteq [0, 1)$ and $\sup_t \beta_t < 1$. The extrapolation step is done by $y^t = x^t + \beta_t(x^t - x^{t-1})$ where the previous iteration x^{t-1} is incorporated. With these preparations, we now give our algorithmic framework, i.e., the Algorithm 1. Henceforth, we will consider the proposed Algorithm 1 with efficient preconditioners for solving the problem.

Algorithm 1 Preconditioned difference-of-convex algorithm with extrapolation (preDCA_e) for $\arg \min_x F(x) = f(x) + P_1(x) - P_2(x)$

$x^0 \in \text{dom } P_1$, $\{\beta_t\} \subseteq [0, 1)$, with $\sup_t \beta_t < 1$. Set $x^{-1} = x^0$.
Iterate the following steps for $t = 0, 1, \dots$,

$$\xi^t \in \partial P_2(x^t), \quad (2.6)$$

$$y^t = x^t + \beta_t(x^t - x^{t-1}) \quad (2.7)$$

$$x^{t+1} = \arg \min_y \left\{ \langle \nabla f(y^t) - \xi^t, y \rangle + \frac{1}{2} \|y - y^t\|_M^2 + P_1(y) \right\}. \quad (2.8)$$

Unless some stopping criterion is satisfied, stop

Supposing the Lipschitz constant of f in Algorithm 1 is L , if choosing $M = L\mathbf{I}$ with \mathbf{I} denoting the identity operator (or the identity matrix when vectoring \mathbf{x}), Algorithm 1 reduces to the proximal extrapolation DCA proposed in [39] with different conditions on P_1 and P_2 . We employ the metric induced by M , which can bring out great flexibility to deal with the linear system with efficient

preconditioners. Let's take the following Lemma 2 for example to illustrate our motivation, where we can reformulate (2.8) as the classical preconditioned iteration [36].

Lemma 2 *With appropriately chosen linear operator $M \geq L_0 \mathbf{I}$ with positive constant $L_0 \geq L$, the iteration (2.8) actually can be reformulated as the following classical preconditioned iteration*

$$x^{t+1} := y^t + M_p^{-1}[b^t - Ty^t], \quad (2.9)$$

where

$$b^t = L_0 y^t - \nabla f(y^t) + \xi^t, \quad T = L_0 \mathbf{I} - \mu \Delta, \quad M_p = M - \mu \Delta \geq T.$$

Proof Denote $b_1^t = \xi^t - \nabla f(y^t)$. By the structure of P_1^A or P_1^I in (1.1), we see

$$M(y - y^t) - \mu \Delta y - b_1^t = 0.$$

We thus have

$$\begin{aligned} x^{t+1} &= (M - \mu \Delta)^{-1}(b_1^t + My^t) \\ &= (M - \mu \Delta)^{-1}((M - \mu \Delta)y^t + b_1^t + \mu \Delta y^t) \\ &= y^t + (M - \mu \Delta)^{-1}[b_1^t + L_0 y^t - (L_0 \mathbf{I} - \mu \Delta)y^t], \\ &= y^t + (M - \mu \Delta)^{-1}[b^t - (L_0 \mathbf{I} - \mu \Delta)y^t], \end{aligned} \quad (2.10)$$

which leads to (2.9) with notation $M_p := M - \mu \Delta$. M_p is actually a preconditioner for T to solve the following linear equation

$$Tx = b^t. \quad (2.11)$$

□

The following remark will give more interpretation of the preconditioned iteration (2.9).

Remark 1 Suppose the discretization of the operator $T = L_0 \mathbf{I} - \mu \Delta$ in Lemma 2 is $D - E - E^*$ (still denoting it as T and using Δ as the discretized Δ) where D is the diagonal part, $-E$ represents the strict lower triangular part and E^* is the transpose of E . If choosing M_p as the symmetric Gauss-Seidel preconditioner for T , it is well-known that [36] (chapter 4.1) (or [6])

$$M_p = T + E^* D^{-1} E.$$

By Lemma 2, since $M_p = (M - \mu \Delta)$, we thus have the explicit form of M

$$M = M_p + \mu \Delta = T + E^* D^{-1} E + \mu \Delta = T + E^* D^{-1} E + L_0 \mathbf{I} - (L_0 \mathbf{I} - \mu \Delta) = E^* D^{-1} E + L_0 \mathbf{I}.$$

We also see $M \geq L_0 \mathbf{I}$ as in Lemma 2. However, we do not need to calculate the explicit form of M or M_p^{-1} , since the update (2.9) is exactly the one time symmetric Gauss-Seidel iteration for the linear equation $Ty = b^t$ [36]. This means that x^{t+1} as in (2.9) is also equivalent to (2.8) through one time symmetric Gauss-Seidel iteration.

For image denosing problem, with $f(x) = \|x - x_0\|_2^2/2$ with Lipschitz constant 1, if we choose $L_0 = \mathbf{I}$ in Lemma 2, the linear equation (2.11) coincides with the original linear equation of DCA (2.5). For image deblurring problem, one possible choice is that we can still use algorithm 1 with $f(x) = \|Ax - x_0\|_2^2/2$, where the symmetric Gauss-Seidel preconditioners can still be employed for the corresponding perturbed Laplacian equation with using $\nabla f(y^t)$ explicitly in (2.8). Here, we provide another choice. Taking the (ATQ) for example, letting

$$f = 0, \quad P_1(y) = \|Ay - x_0\|_2^2/2 + P_1^A(y), \quad P_2(y) = P_2^A(y), \quad (2.12)$$

we have the following proposition, whose proof is completely similar to Lemma 2 and is thus omitted.

Proposition 1 *With appropriately chosen linear operator $M \geq L_0\mathbf{I}$ with positive constant $L_0 \geq L$ and the data in (2.12), the iteration (2.8) in Algorithm 1 can be reformulated as the following classical preconditioned iteration*

$$x^{t+1} := y^t + M_p^{-1}[b^t - Ty^t], \quad (2.13)$$

where

$$b^t = L_0y^t + A^*x_0 + \xi^t, \quad T = L_0\mathbf{I} + A^*A - \mu\Delta, \quad M_p = M + A^*A - \mu\Delta \geq T.$$

The condition $M \geq L_0\mathbf{I}$ comes from the positive definite requirement of M , which is important for the following convergence analysis. However, we can choose very small L_0 for the deblurring problem and T can thus approximate the original linear system (2.5). Throughout this paper, if $f = 0$ in (2.12) with Lipschitz constant $L = 0$, we further assume $M \geq L_0\mathbf{I}$ with constant $L_0 > 0$.

With Lemma 2, Remark 1, and Proposition 1, it can be seen that one can cooperate the classical preconditioned iteration into the DCA framework through the proximal mapping with metric. We thus can deal with linear systems with powerful tools from the classical preconditioning techniques for linear algebraic equations. Now let's turn to the KL analysis for the convergence with our preconditioning framework. We begin with the KL exponent of the quadratic functions with an elementary proof.

Lemma 3 *The quadratic function $q(x) = \frac{1}{2}x^TQx - u^Tx + s$ is a KL function with KL exponent of $\frac{1}{2}$, where Q is a symmetric positive semidefinite matrix. Moreover, supposing that the minimal positive eigenvalue of M is λ_M , then there exist small positive ε and η , such that for any x satisfying $|x - \bar{x}| \leq \varepsilon$ and $q(\bar{x}) < q(x) < q(\bar{x}) + \eta$, we have*

$$q(x) - q(\bar{x}) = |q(x) - q(\bar{x})| \leq \frac{1}{2\lambda_M} |\nabla q(x)|^2.$$

Proof First, noting that $\frac{1}{2}x^TQx - u^Tx + s$ and $\frac{1}{2}x^TQx - u^Tx$ have the same KL exponent, we just need to prove the case of the function $q(x) = \frac{1}{2}x^TQx - u^Tx$ without loss of generality. We first consider the case \bar{x} such that $\nabla q(x)|_{x=\bar{x}} = 0$, i.e., $Q\bar{x} = u$. Supposing $\lambda_1 \geq \lambda_2 \geq \dots \geq \lambda_n \geq 0$ are the eigenvalues of Q , we know $\lambda_M = \min\{\lambda_i, \lambda_i > 0\}$ by assumption. There exists an orthogonal

matrix P such that $Q = P^{-1}\text{Diag}[\lambda_1, \dots, \lambda_n]P$. Furthermore,

$$\begin{aligned} |q(x) - q(\bar{x})| &= \left| \frac{1}{2} \langle Q(x - \bar{x}), x - \bar{x} \rangle \right| \\ &= \frac{1}{2} (x - \bar{x})^T P^{-1} \begin{pmatrix} \lambda_1 & & \\ & \ddots & \\ & & \lambda_n \end{pmatrix} P(x - \bar{x}) \leq \frac{1}{2\lambda_M} (x - \bar{x})^T P^{-1} \begin{pmatrix} \lambda_1^2 & & \\ & \ddots & \\ & & \lambda_n^2 \end{pmatrix} P(x - \bar{x}) \\ &= \frac{1}{2\lambda_M} \langle Q(x - \bar{x}), Q(x - \bar{x}) \rangle = \frac{1}{2\lambda_M} \langle Qx - u, Qx - u \rangle = \frac{1}{2\lambda_M} |\nabla q(x)|^2. \end{aligned}$$

Now, let's turn to the case $|\nabla q(\bar{x})| = |Q\bar{x} - u| = \delta_0 > 0$. Supposing $|x - \bar{x}| \leq \varepsilon$, we see

$$\begin{aligned} |q(x) - q(\bar{x})| &= \left| \frac{1}{2} x^T Qx - u^T x - \frac{1}{2} \bar{x}^T Q\bar{x} + u^T \bar{x} \right| \\ &= \left| \left\langle \frac{1}{2} (x - \bar{x})^T Q(x - \bar{x}) + \langle Q\bar{x} - u, x - \bar{x} \rangle \right. \right| \\ &\leq \frac{1}{2} \|Q\| \varepsilon^2 + \delta_0 \varepsilon. \end{aligned} \tag{2.14}$$

For $|\nabla q(x)|^2$, we have

$$\begin{aligned} |\nabla q(x)|^2 &= |Qx - u|^2 = |Qx - Q\bar{x} + Q\bar{x} - u|^2 \\ &= |Qx - Q\bar{x}|^2 + 2\langle Q(x - \bar{x}), Q\bar{x} - u \rangle + |Q\bar{x} - u|^2 \geq \delta_0^2 - \|Q\|^2 \varepsilon^2 - 2\delta_0 \|Q\| \varepsilon. \end{aligned} \tag{2.15}$$

To obtain $|q(x) - q(\bar{x})| \leq \frac{1}{2\lambda_M} |\nabla q(x)|^2$, one can choose

$$(\delta_0^2 - \|Q\|^2 \varepsilon^2 - 2\delta_0 \|Q\| \varepsilon) \frac{1}{2\lambda_M} \geq \frac{\delta_0^2}{2} \frac{1}{2\lambda_M} \geq \frac{1}{2} \|Q\| \varepsilon^2 + \delta_0 \varepsilon,$$

which leads to

$$\varepsilon \leq \Delta_0 := \min \left(\frac{\delta_0}{\|Q\|}, \frac{\delta_0}{\|Q\|} \left(\sqrt{\frac{\|Q\|}{2\lambda_M} + 1} - 1 \right) \right).$$

We thus have $|q(x) - q(\bar{x})| \leq \frac{1}{2\lambda_M} |\nabla q(x)|^2$ for all $|x - \bar{x}| \leq \Delta_0$. The proof is complete. \square

Remark 2 Lemma 3 can be seen as a special case of Corollary 5.1 of [24], which originated from [27] for the convex quadratic problem.

We now discuss the KL exponent of the truncated quadratic regularization functional (ITQ) and (ATQ). We will employ the recent study on KL analysis of the functions which can be written as minimization of a finite number of KL functions with KL exponent 1/2; see [24]. Let's turn to the following theorem.

Theorem 1 *Assuming the linear operators $A : X \rightarrow Y_0 = \mathbb{R}^{m_0 \times n_0}$, $K_l : X \rightarrow Y_l = \mathbb{R}^{m_l \times n_l \times c_l}$, $l = 1, \dots, k$ are linear, bounded operators and μ_l, τ_l are positive parameters, then the KL exponent of the following general truncated quadratic regularization functional $F(\mathbf{x})$ is 1/2,*

$$F(\mathbf{x}) = \frac{\|A\mathbf{x} - \mathbf{x}_0\|_2^2}{2} + \sum_{l=1}^k \sum_{i=1}^{m_l} \sum_{j=1}^{n_l} \frac{\mu_l}{2} \min(|(K_l \mathbf{x})_{i,j}|^2, \tau_l). \tag{2.16}$$

Proof Let's first vectorize \mathbf{x} and \mathbf{x}_0 as the column vector $x \in \mathbb{R}^{mn}$ and $x_0 \in \mathbb{R}^{m_0n_0}$ correspondingly. We will still use $A, K_l, l = 1, \dots, k$ as the discrete matrix versions of the corresponding linear operators. The equation (2.16) then becomes

$$F(x) = \frac{\|Ax - x_0\|_2^2}{2} + \sum_{l=1}^k \sum_{i=1}^{m_l n_l} \frac{\mu_l}{2} \min(|(K_l x)_i|^2, \tau_l), \quad (2.17)$$

where $(K_l x)_i$ denote the i -th component of $K_l x$. Note the fact that

$$\min(a, b) + \min(c, d) = \min(a + c, a + d, b + c, b + d), \quad \forall a, b, c, d \in \mathbb{R}.$$

Similarly, for the summation with $N := \sum_{l=1}^k m_l n_l$ terms with each term of the form $\min(|(K_l x)_i|^2, \tau_l)$ as in (2.17), we can rewrite $F(x)$ as follows

$$F(x) = \frac{\|Ax - x_0\|_2^2}{2} + \min_{1 \leq i \leq 2^N} P_i(x). \quad (2.18)$$

$P_i(x)$ comes from summing the selected term $|(K_l x)_i|^2$ or τ_l from $\min(|(K_l x)_i|^2, \tau_l)$ for $l = 1, \dots, k$ and $i = 1, \dots, m_l n_l$. For example, we can choose

$$P_1(x) = \sum_{l=1}^k \sum_{i=1}^{m_l n_l} \tau_l, \quad P_2(x) = \sum_{l=1}^k \sum_{i=1}^{m_l n_l} |(K_l x)_i|^2.$$

All the other $P_i(x)$ with $i = 3, \dots, 2^N$ can be chosen similarly. Furthermore, it can be readily checked that each $P_i(x), i = 1, \dots, 2^N$, is a convex quadratic function. It is straightforward that (2.18) can be written as

$$F(x) = \min_{1 \leq i \leq 2^N} F_i(x), \quad F_i(x) := \frac{\|Ax - x_0\|_2^2}{2} + P_i(x), \quad i = 1, \dots, 2^N. \quad (2.19)$$

Actually, we can reformulate each $F_i(x)$ in the form of quadratic function as in Lemma 3. Taking the function $F_2(x)$ for example, let

$$A = [A/\sqrt{2}, K_{1,1}, \dots, K_{1,m_1 n_1}, \dots, K_{l,1}, \dots, K_{l,m_l n_l}, \dots, K_{k,1}, \dots, K_{k,m_k n_k}]^T,$$

$$b = [x_0/\sqrt{2}, 0, \dots, 0]^T \in \mathbb{R}^{N_0}, \quad N_0 := m_0 n_0 + \sum_{l=1}^k m_l n_l c_l,$$

where $K_{i_1, i_2} x = (K_{i_1} x)_{i_2}$, $i_1 = 1, \dots, k$, and $i_2 = 1, \dots, m_{i_1} n_{i_1}$. We can thus rewrite $F_2(x)$ as follows

$$P_2(x) = \|Ax - b\|_2^2,$$

which is clearly a quadratic function. Since each $F_i(x)$ is a quadratic function as in Lemma 3, then each $F_i(x)$ has KL exponent 1/2 by Lemma 3. With [24] (Theorem 3.1) and noting $F(x)$ is a continuous function, we conclude that $F(x)$ is a KL function with an exponent 1/2, since it can be written as minimization of $F_i(x)$ with KL exponent of 1/2 in (2.19). \square

Remark 3 For the isotropic model (ITQ), we can choose $m_0 = m, n_0 = n, K_1 = [\nabla_1, \nabla_2]$ with $m_1 = n, n_1 = n, c_1 = 2$ and $k = 1$ as in (2.16). For the anisotropic model (ATQ), we can choose $m_0 = m, n_0 = n, K_1 = \nabla_1$ and $K_2 = \nabla_2$ with $m_1 = m_2 = m, n_1 = n_2 = n, c_1 = c_2 = 1$ and $k = 2$ as in (2.16).

Henceforth, we will make extensive use of the following auxiliary function

$$E(x, y) = f(x) + P(x) + \frac{1}{2}\|x - y\|_M^2 = F(x) + \frac{1}{2}\|x - y\|_M^2. \quad (2.20)$$

Let's calculate the exponent of KL inequality of the auxiliary function $E(x, y)$ in (2.20) at the stationary point. We do this through the relationship between the original function $F(x)$ and the auxiliary function $E(x, y)$.

Lemma 4 *If a proper closed function $F(x)$ has the KL property at a stationary point \bar{x} with an exponent of $\frac{1}{2}$, then the auxiliary function $E(x, y) = F(x) + \frac{1}{2}\|x - y\|_M^2$ has the KL property at the stationary point (\bar{x}, \bar{x}) with the exponent of $\frac{1}{2}$.*

Proof Because \bar{x} is a stationary point of $F(x)$, we have $0 \in \partial F(\bar{x})$. Supposing $0 \in \partial E(\bar{x}, \bar{y}) = (\partial F(\bar{x}) + M(\bar{x} - \bar{y}), M(\bar{y} - \bar{x}))^T$, we have $\bar{x} = \bar{y}$ by $M \geq L_0 \mathbf{I}$. Since F has the KL property at \bar{x} with the exponent $\frac{1}{2}$, there exist c_1, ϵ and $\eta > 0$ such that

$$(F(x) - F(\bar{x})) \leq c_1 \text{dist}^2(0, \partial F(x)), \quad (2.21)$$

whenever $x \in \text{dom } \partial F(x)$, $\|x - \bar{x}\| \leq \epsilon$ and $F(\bar{x}) < F(x) < F(\bar{x}) + \eta$. We thus have

$$\begin{aligned} |E(x, y) - E(\bar{x}, \bar{x})| &\leq |F(x) - F(\bar{x})| + \frac{1}{2}\|x - y\|_M^2 \\ &\leq c_1 \text{dist}^2(0, \partial F(x)) + \frac{1}{2}\|x - y\|_M^2 \end{aligned} \quad (2.22)$$

for any (x, y) satisfying $x \in \text{dom } \partial F$, $\|x - \bar{x}\| \leq \epsilon$, $\|y - \bar{x}\| \leq \epsilon$ and $E(\bar{x}, \bar{x}) < E(x, y) < E(\bar{x}, \bar{x}) + \eta$. Furthermore, if there exists a positive constant c_2 such that

$$\begin{aligned} c_1 \text{dist}^2(0, \partial F(x)) + \frac{1}{2}\|x - y\|_M^2 &\leq c_2 \text{dist}^2(0, \partial E(x, y)) \\ &= c_2 \text{dist}^2((0, 0)^T, (\partial F(x) + M(x - y), M(y - x))^T), \end{aligned} \quad (2.23)$$

we get the lemma. For any $\epsilon > 0$, we have

$$\begin{aligned} \text{dist}^2(0, \partial E(x, y)) &= 2\|M(y - x)\|^2 + \inf_{\xi \in \partial F(x)} (\|\xi\|^2 + \langle \xi, x - y \rangle_M) \\ &\geq 2\|M(y - x)\|^2 + \inf_{\xi \in \partial F(x)} \left[\|\xi\|^2 - (\alpha\|\xi\|^2 + \frac{1}{\alpha}\|M(x - y)\|^2) \right] \\ &= (2 - \frac{1}{\alpha})\|M(y - x)\|^2 + (1 - \alpha) \text{dist}^2(0, \partial F(x)) \\ &\geq (2 - \frac{1}{\alpha})\lambda_M\|y - x\|_M^2 + (1 - \alpha) \text{dist}^2(0, \partial F(x)) \end{aligned} \quad (2.24)$$

where the first inequality follows from the inequality $ab \geq -(\alpha a^2 + \frac{1}{\alpha} b^2)$, $\forall \alpha > 0$ and λ_M is the minimum positive eigenvalue of M as before. Setting $\frac{1}{2} < \alpha < 1$, we have $1 - \alpha > 0$ and $2 - \frac{1}{\alpha} > 0$. With (2.22) and (2.24), to obtain (2.23), one can fix c_2 as follows

$$\frac{1}{2} \leq c_2(2 - \frac{1}{\alpha})\lambda_M, \quad c_1 \leq c_2(1 - \alpha) \Rightarrow c_2 \geq \max\left(\frac{c_1}{1 - \alpha}, \frac{\alpha}{(4\alpha - 2)\lambda_M}\right) \geq 0. \quad (2.25)$$

We thus get

$$|E(x, y) - E(\bar{x}, \bar{x})| \leq c_2 \text{dist}^2(0, \partial E(x, y)), \quad (2.26)$$

and the lemma follows. \square

2.2 Global convergence and local convergence rate

Recall that \bar{x} is a stationary point of F if $0 \in \partial F(\bar{x})$. We will first study a property of the iteration (2.8). We further assume F is level-bounded (see Definition 1.8 [35]), i.e., $\text{lev}_{\leq \alpha} F := \{x : F(x) \leq \alpha\}$ is bounded (or possibly empty). We employ the similar idea in [39] with different conditions on P_1 and P_2 here.

Proposition 2 *The right hand-side of (2.8): $g(x) := \langle \nabla f(y^t) - \xi^t, x \rangle + \frac{1}{2} \|x - y^t\|_M^2 + P_1(x)$ is a strongly convex function. Moreover, $g(x^{t+1}) \leq g(x^t) - \frac{1}{2} \|x^{t+1} - x^t\|_M^2$ when x^{t+1} is a stationary point of $g(x)$.*

Proof For any $\xi_1 \in \partial P_1(x)$, by the convexity of $\frac{1}{2} \|x - y^t\|_M^2$ and $P_1(x)$ on x , we have

$$\begin{aligned} g(y) - g(x) &= \langle \nabla f(y^t) - \xi^t, y - x \rangle + \frac{1}{2} \|y - y^t\|_M^2 - \frac{1}{2} \|x - y^t\|_M^2 + P_1(y) - P_1(x) \\ &\geq \langle \nabla f(y^t) - \xi^t, y - x \rangle + \frac{1}{2} \|y - x\|_M^2 + \langle x - y^t, y - x \rangle_M + \langle \xi_1, y - x \rangle \\ &= \langle \nabla f(y^t) - \xi^t + M(x - y^t) + \xi_1, y - x \rangle + \frac{1}{2} \|y - x\|_M^2 \\ &\geq \langle \nabla f(y^t) - \xi^t + M(x - y^t) + \xi_1, y - x \rangle + \frac{L}{2} \|y - x\|^2, \quad \forall x, y \in \text{dom } g. \end{aligned} \quad (2.27)$$

Since

$$\nabla f(y^t) - \xi^t + M(x - y^t) + \xi_1 \in \partial g(x),$$

we see $g(x)$ is a strongly convex function with a modulus that is not less than L_0 . Setting $x = x^{t+1}$ and $y = x^t$, by the fact that $0 \in \partial g(x)|_{x = x^{t+1}}$, according to (2.8), together with (2.27), we have

$$g(x^{t+1}) \leq g(x^t) - \frac{1}{2} \|x^{t+1} - x^t\|_M^2. \quad (2.28)$$

□

We will first show that the sequence $\{x^t\}$ generated by the proposed algorithm 1 converges to a stationary point of $E(x, y)$.

Theorem 2 *Let x^t be a sequence generated by preDCA_e for solving the minimization problem (ITQ) or (ATQ). Then the following statements hold:*

- (i) $\lim_{t \rightarrow \infty} \|x^{t+1} - x^t\|_M = 0$,
- (ii) *The limit $\lim_{k \rightarrow \infty} E(x^t, x^{t-1}) =: \zeta$ exists and $E \equiv \zeta$ on Υ . Henceforth, we denote Υ as the set of accumulation points of the sequence (x^t, x^{t-1}) .*

Proof We first prove (i). By Proposition 2, we can get

$$\begin{aligned} &\langle \nabla f(y^t) - \xi^t, x^t \rangle + \frac{1}{2} \|x^{t+1} - y^t\|_M^2 + P_1(x^{t+1}) \\ &\leq \langle \nabla f(y^t) - \xi^t, x^{t+1} \rangle + \frac{1}{2} \|x^t - y^t\|_M^2 + P_1(x^t) - \frac{1}{2} \|x^{t+1} - x^t\|_M^2. \end{aligned} \quad (2.29)$$

On the other hand, since ∇f is Lipschitz continuous with a modulus of L , we have

$$\begin{aligned}
f(x^{t+1}) + P(x^{t+1}) &\leq f(y^t) + \langle \nabla f(y^t), x^{t+1} - y^t \rangle + \frac{L}{2} \|x^{t+1} - y^t\|^2 + P_1(x^{t+1}) - P_2(x^{t+1}) \\
&\leq f(y^t) + \langle \nabla f(y^t), x^{t+1} - y^t \rangle + \frac{1}{2} \|x^{t+1} - y^t\|_M^2 + P_1(x^{t+1}) - P_2(x^{t+1}) \\
&\leq f(y^t) + \langle \nabla f(y^t), x^{t+1} - y^t \rangle + \frac{1}{2} \|x^{t+1} - y^t\|_M^2 + P_1(x^{t+1}) - P_2(x^t) - \langle \xi^t, x^{t+1} - x^t \rangle \\
&\leq f(y^t) + \langle \nabla f(y^t), x^t - y^t \rangle + \frac{1}{2} \|x^t - y^t\|_M^2 + P_1(x^t) - P_2(x^t) - \frac{1}{2} \|x^{t+1} - x^t\|_M^2 \\
&\leq f(x^t) + P(x^t) + \frac{1}{2} \|x^t - y^t\|_M^2 - \frac{1}{2} \|x^{t+1} - x^t\|_M^2,
\end{aligned} \tag{2.30}$$

where the second inequality follows from $M \geq L_0 \mathbf{I} \geq L \mathbf{I}$, the third one comes from the fact that $\xi^t \in \partial P_2(x^t)$, the fourth inequality follows from (2.28) and the fifth one by the convexity of f . From (2.30), we have

$$f(x^{t+1}) + P(x^{t+1}) \leq f(x^t) + P(x^t) + \frac{1}{2} \beta_t^2 \|x^t - x^{t-1}\|_M^2 - \frac{1}{2} \|x^{t+1} - x^t\|_M^2.$$

Then, we can obtain that

$$\begin{aligned}
\frac{1}{2} (1 - \beta_t^2) \|x^t - x^{t-1}\|_M^2 &\leq \left[f(x^t) + P(x^t) + \frac{1}{2} \|x^t - x^{t-1}\|_M^2 \right] \\
&\quad - \left[f(x^{t+1}) + P(x^{t+1}) + \frac{1}{2} \|x^{t+1} - x^t\|_M^2 \right] = E(x^t, x^{t-1}) - E(x^{t+1}, x^t).
\end{aligned} \tag{2.31}$$

Since $\beta_t \in [0, 1)$, we see from (2.31) that $f(x^t) + P(x^t) + \frac{1}{2} \|x^t - x^{t-1}\|_M^2$ is nonincreasing. We can thus get that

$$f(x^t) + P(x^t) \leq f(x^t) + P(x^t) + \frac{1}{2} \|x^t - x^{t-1}\|_M^2 \leq f(x^0) + P(x^0), \quad \forall t \geq 0,$$

which shows that x^t is bounded by the level-boundedness of F (Definition 1.8 of [35] and [39]) and $F(x) \geq 0$. Then summing up both sides of (2.31) from $t = 0$ to ∞ , we obtain

$$\begin{aligned}
\frac{1}{2} \sum_{t=0}^{\infty} (1 - \beta_t^2) \|x^t - x^{t-1}\|_M^2 &\leq f(x^0) + P(x^0) - \liminf_{t \rightarrow \infty} \left[f(x^{t+1}) + P(x^{t+1}) + \frac{1}{2} \|x^{t+1} - x^t\|_M^2 \right] \\
&\leq f(x^0) + P(x^0) < \infty.
\end{aligned}$$

Since $\sup_t \beta_t < 1$, we deduce from the above inequation that $\sum_{t=1}^{\infty} \|x^t - x^{t-1}\|_M^2 < \infty$ and $\lim_{t \rightarrow \infty} \|x^{t+1} - x^t\|_M^2 = 0$. This proves (i).

Now we prove (ii), it can be seen that the sequence $E(x^t, x^{t-1})$ is nonincreasing form (2.31). Together with the fact that \mathcal{Y} is a nonempty compact set due to x^t is bounded, we conclude that $\zeta := \lim_{k \rightarrow \infty} E(x^t, x^{t-1})$ exists. Now, let's show $E \equiv \zeta$ on \mathcal{Y} . Taking any $(\bar{x}, \bar{x}) \in \mathcal{Y}$, there exists a convergent subsequence (x^{t_i}, x^{t_i-1}) such that $\lim_{i \rightarrow \infty} (x^{t_i}, x^{t_i-1}) = (\bar{x}, \bar{x})$. Using the fact that x^{t_i} is the minimizer of the subproblem in (2.8), we have

$$\begin{aligned}
P_1(x^{t_i}) + \langle \nabla f(y^{t_i-1}) - \xi^{t_i-1}, x^{t_i} \rangle + \frac{1}{2} \|x^{t_i} - y^{t_i-1}\|_M^2 \\
\leq P_1(\bar{x}) + \langle \nabla f(y^{t_i-1}) - \xi^{t_i-1}, \bar{x} \rangle + \frac{1}{2} \|\bar{x} - y^{t_i-1}\|_M^2.
\end{aligned}$$

Rearranging terms above, we obtain

$$P_1(x^{t_i}) + \langle \nabla f(y^{t_i-1}) - \xi^{t_i-1}, x^{t_i} - \bar{x} \rangle + \frac{1}{2} \|x^{t_i} - y^{t_i-1}\|_M^2 \leq P_1(\bar{x}) + \frac{1}{2} \|\bar{x} - y^{t_i-1}\|_M^2. \quad (2.32)$$

Furthermore, we observe

$$\begin{aligned} \|\bar{x} - y^{t_i-1}\|_M &= \|\bar{x} - x^{t_i} + x^{t_i} - y^{t_i-1}\|_M \leq \|\bar{x} - x^{t_i}\|_M + \|x^{t_i} - y^{t_i-1}\|_M \\ &= \|\bar{x} - x^{t_i}\|_M + \|x^{t_i} - x^{t_i-1} - \beta_{t_i-1}(x^{t_i-1} - x^{t_i-2})\|_M \\ &\leq \|\bar{x} - x^{t_i}\|_M + \|x^{t_i} - x^{t_i-1}\|_M + \|x^{t_i-1} - x^{t_i-2}\|_M. \end{aligned}$$

Since $\|x^{t+1} - x^t\|_M \rightarrow 0$ and $\lim_{i \rightarrow \infty} x^{t_i} = \bar{x}$, we have

$$\|\bar{x} - y^{t_i-1}\|_M \rightarrow 0 \quad \text{and} \quad \|x^{t_i} - y^{t_i-1}\|_M \rightarrow 0.$$

Moreover, with (2.32), we obtain

$$\begin{aligned} \zeta &= \lim_{i \rightarrow \infty} f(x^{t_i}) + P(x^{t_i}) \\ &= \lim_{i \rightarrow \infty} f(x^{t_i}) + P(x^{t_i}) + \langle \nabla f(y^{t_i-1}) - \xi^{t_i-1}, x^{t_i} - \bar{x} \rangle + \frac{1}{2} \|x^{t_i} - y^{t_i-1}\|_M^2 \\ &\leq \limsup_{i \rightarrow \infty} f(x^{t_i}) + P_1(\bar{x}) - P_2(x^{t_i}) + \frac{1}{2} \|\bar{x} - y^{t_i-1}\|_M^2 = F(\bar{x}). \end{aligned}$$

Since F is lower semicontinuous, we have

$$F(\bar{x}) \leq \liminf_{i \rightarrow \infty} F(x^{t_i}) = \lim_{i \rightarrow \infty} F(x^{t_i}) = \zeta. \quad (2.33)$$

Consequently, $F(\bar{x}) = \liminf_{i \rightarrow \infty} F(x^{t_i}) = \zeta$. Noting that for any $(\bar{x}, \bar{x}) \in \mathcal{Y}$, we have $E(\bar{x}, \bar{x}) = F(\bar{x}) = \zeta$. We thus conclude $E \equiv \zeta$ on \mathcal{Y} and (ii) follows. \square

Theorem 3 *Any accumulation point of x^t is a stationary point of F . Furthermore, we have $\sum_{k=1}^{\infty} \|x^k - x^{k-1}\| \leq \infty$.*

Proof With the same assumption of Theorem 2, let \bar{x} be an accumulation of x^t . By the first-order optimality condition of the subproblem (2.8), we get

$$-M(x^{t+1} - y^t) \in \nabla P_1(x^{t+1}) + \nabla f(y^t) - \xi^t.$$

With the fact $y^t = x^t + \beta_t(x^t - x^{t-2})$, we obtain that

$$-M[(x^{t+1} - x^t) - \beta_t(x^t - x^{t-2})] \in \nabla P_1(x^{t+1}) + \nabla f(y^t) - \xi^t. \quad (2.34)$$

Because of the convexity of P_2 and the the boundeness of x^t , by passing to a subsequence if necessary, then $\lim_{i \rightarrow \infty} \xi^t$ exists without loss of generality, which belongs to $\partial P_2(\bar{x})$ due to the closedness of ∂P_2 (Theorem 8.6 [35]). Using the fact that $\|x^{t+1} - x^t\|_M^2 \rightarrow 0$ from Theorem 2 (ii) together with the closedness of ∇P_1 and ∇f , we get upon passing to the limit in (2.34) that

$$0 \in \nabla P_1(\bar{x}) + \nabla f(\bar{x}) - \partial P_2(\bar{x}).$$

Then, considering the subdifferential of the function $E(x, y)$ at the point (x^t, x^{t-1}) , we have

$$\partial E(x^t, x^{t-1}) = (\nabla f(x^t) + \nabla P_1(x^t) + M(x^t - x^{t-1}) - \partial P_2(x^t), -M(x^t - x^{t-1}))^T. \quad (2.35)$$

On the other hand, with (2.34) and the fact $\xi^t \in \partial P_2(x^t)$, we have

$$\begin{aligned} & (M(x^t - x^{t+1} + (1 + \beta_t)(x^t - x^{t-1})) + \nabla f(x^t) - \nabla f(y^t) + \nabla P_1(x^t) - \nabla P_1(x^{t+1}), \\ & - M(x^t - x^{t-1}))^T \in \partial E(x^t, x^{t-1}). \end{aligned}$$

Together with the fact that $\nabla f, \nabla P_1$ is Lipschitz continuous on a bounded set and $M \geq L\mathbf{I}$, we see that there exists $C_0 > 0$ such that

$$\begin{aligned} \text{dist}((0, 0), \partial E(x^t, x^{t-1})) & \leq C_0(\|x^t - x^{t-1}\|_M + \|x^{t+1} - x^t\|_M) \\ & \leq C(\|x^t - x^{t-1}\| + \|x^{t+1} - x^t\|), \end{aligned} \quad (2.36)$$

where the constant C depending on M and C_0 . We rewrite (2.31) as

$$E(x^t, x^{t-1}) - E(x^{t+1}, x^t) \geq D_0 \|x^t - x^{t-1}\|_M^2 \geq D \|x^t - x^{t-1}\|^2. \quad (2.37)$$

Then, we first consider the case that there exists a $t > 0$ such that $E(x^t, x^{t-1}) = \zeta$. Since $E(x^t, x^{t-1})$ is decreasing with the limit ζ , we thus have $E(\bar{x}^t, \bar{x}^{t-1}) = \zeta$ for any $\bar{t} > t$. Hence, $\sum_{t=0}^{\infty} \|x^t - x^{t-1}\|_M < \infty$ follows easily. We next consider the case that $E(x^t, x^{t-1}) > \zeta, \forall t > 0$. Since E is a KL function and $E \equiv \zeta$ on \mathcal{Y} , by Lemma 1, there exist an $\epsilon > 0$ and a continuous concave function ψ with $a > 0$ such that

$$\psi'(E(x, y) - \zeta) \text{dist}((0, 0), \partial E(x, y)) \geq 1, \quad \forall (x, y) \in U, \quad (2.38)$$

where $U = \{(x, y) \in \mathbb{R}^n \times \mathbb{R}^n : \text{dist}((x, y), \mathcal{Y}) < \epsilon\} \cap \{(x, y) \in \mathbb{R}^n \times \mathbb{R}^n : \zeta < E(x, y) < \zeta + a\}$. Moreover, we can get that there exists $T > 0$ such that

$$\psi'(E(x^t, x^{t-1}) - \zeta) \cdot \text{dist}((0, 0), \partial E(x^t, x^{t-1})) \geq 1, \quad \forall t \geq T. \quad (2.39)$$

Due to $\lim_{t \rightarrow \infty} \text{dist}((x^t, x^{t-1}), \mathcal{Y}) = 0$, there thus exists $T_1 > 0$ such that $\text{dist}((x^t, x^{t-1}), \mathcal{Y}) < \epsilon$ whenever $t \geq T_1$. From the concavity of ψ , we see that

$$\begin{aligned} & [\psi(E(x^t, x^{t-1}) - \zeta) - \psi(E(x^{t+1}, x^t) - \zeta)] \cdot \text{dist}((0, 0), \partial E(x^t, x^{t-1})) \\ & \geq \psi'(E(x^t, x^{t-1}) - \zeta) \cdot \text{dist}((0, 0), \partial E(x^t, x^{t-1})) \cdot [E(x^t, x^{t-1}) - E(x^{t+1}, x^t)] \\ & \geq E(x^t, x^{t-1}) - E(x^{t+1}, x^t). \end{aligned}$$

Combining this with (2.36) and (2.37), we can get that for any $t \geq T$,

$$\begin{aligned} \|x^t - x^{t-1}\|^2 & \leq \frac{C}{D} [\psi(E(x^t, x^{t-1}) - \zeta) - \psi(E(x^{t+1}, x^t) - \zeta)] \\ & \quad \cdot (\|x^t - x^{t-1}\| + \|x^{t-1} - x^{t-2}\|). \end{aligned}$$

Moreover, we can see further that (by the inequality $a \leq \sqrt{cd} \Rightarrow a \leq c + \frac{d}{4}$ for $a, b, c \geq 0$)

$$\begin{aligned} \frac{1}{2} \|x^t - x^{t-1}\| & \leq \frac{C}{D} [\psi(E(x^t, x^{t-1}) - \zeta) - \psi(E(x^{t+1}, x^t) - \zeta)] \\ & \quad + \frac{1}{4} (\|x^{t-1} - x^{t-2}\| - \|x^t - x^{t-1}\|). \end{aligned} \quad (2.40)$$

Summing up the above relation from $t = T$ to ∞ , we have

$$\sum_{t=T}^{\infty} \|x^t - x^{t-1}\| \leq \frac{2C}{D} \psi(E(x^T, x^{T-1}) - \zeta) + \frac{1}{2} \|x^{T-1} - x^{T-2}\| < \infty. \quad (2.41)$$

Thus $\{x^t\}$ is a Cauchy sequence and its global convergence follows. \square

Remark 4 Actually, the proofs in Theorems 2 and 3 have a lot of differences from the proofs in [39]. These are mainly because of two reasons. The first is the proximal term $\|y - y^t\|_M^2/2$ designed for preconditioning which is different from [39] where $M = LI$. The second is the conditions on the functions P_1 and P_2 are different from [39] as mentioned in section 1.

We next consider the convergence rate of the sequence $\{x^t\}$ under the condition that the auxiliary function E is a KL function at the stationary point whose ψ takes the form $\psi(s) = cs^{1-\theta}$ for $\theta = \frac{1}{2}$, which can be guaranteed by Theorem 1 and Lemma 4. This kind of convergence rate analysis is standard; see [1, 2, 24, 39] for more comprehensive analysis. We follow a similar line of arguments for the local convergence analysis based on the KL property.

Theorem 4 *Let x^t be a sequence generated by preDCA_e for solving (ITQ) or (ATQ) and suppose that x^t converges to some \bar{x} . Since E is a KL function with ψ in KL inequality taking the form $\psi(s) = cs^{1-\theta}$ for $\theta = \frac{1}{2}$ and $c > 0$ at the stationary point, then there exist $c_1 > 0, t_0 > 0$ and $\eta \in (0, 1)$ such that $\|x^t - \bar{x}\| < c_1\eta^t$ for $\forall t > t_0$.*

Proof If there exists $t_0 > 0$ such that $E(x^{t_0}, x^{t_0-1}) = \zeta$, then one can show that x^t is finitely convergent as before and the local linear convergence holds trivially. Hence, we only consider the case when $E(x^t, x^{t-1}) > \zeta, \forall t > 0$. Define $\Delta_t = E(x^t, x^{t-1}) - \zeta$ and $S_t = \sum_{i=t}^{\infty} \|x^{i+1} - x^i\|$, where S_t is well-define thanks to Theorem 2 (ii). Then, using (2.40), we have for any $t > T$ that

$$\begin{aligned} S_t &= 2 \sum_{i=t}^{\infty} \frac{1}{2} \|x^{i+1} - x^i\| \leq 2 \sum_{i=t}^{\infty} \frac{1}{2} \|x^i - x^{i-1}\| \\ &\leq 2 \sum_{i=t}^{\infty} \left[\frac{C}{D} [\phi(E(x^i, x^{i-1})) - \zeta) - \phi(E(x^{i+1}, x^i) - \zeta)] + \frac{1}{4} (\|x^{i-1} - x^{i-2}\| - \|x^i - x^{i-1}\|) \right] \\ &\leq \frac{2C}{D} \phi(E(x^t, x^{t-1}) - \zeta) + \frac{1}{2} \|x^{t-1} - x^{t-2}\| \\ &= \frac{2C}{D} \phi(\Delta_t) + \frac{1}{2} (S_{t-2} - S_{t-1}) \leq \frac{2C}{D} \phi(\Delta_t) + \frac{1}{2} (S_{t-2} - S_t), \end{aligned}$$

where the last inequality follows from the fact that S_t is nonincreasing. By (2.39) with $\psi(s) = cs^{\frac{1}{2}}$, for all sufficiently large t ,

$$\frac{c}{2} \Delta_t^{-\frac{1}{2}} \text{dist}((0, 0), \partial E(x^t, x^{t-1})) \geq 1.$$

Rewriting (2.36) by the definition of S_t , we see that for all sufficiently large t ,

$$\text{dist}((0, 0), \partial E(x^t, x^{t-1})) \leq C(S_{t-2} - S_t).$$

We thus can get

$$(\Delta_t)^{\frac{1}{2}} \leq \frac{Cc}{2} (S_{t-2} - S_t).$$

Combining this with $S_t \leq \frac{2C}{D} \phi(\Delta_t) + \frac{1}{2} (S_{t-2} - S_t)$, we see that for all sufficiently large t ,

$$S_t \leq C_1 (S_{t-2} - S_t) + \frac{1}{2} (S_{t-2} - S_t) = (C_1 + \frac{1}{2}) (S_{t-2} - S_t), \quad (2.42)$$

where $C_1 = \frac{c^2 C^2}{D}$. Hence,

$$\|x^t - \bar{x}\| \leq \sum_{i=t}^{\infty} \|x^{i+1} - x^i\| = S_t \leq S_{t_1-2} \eta^{t-t_1+1}, \quad \eta := \sqrt{\frac{2C_1+1}{2C_1+3}}, \quad (2.43)$$

which completes the proof. \square

Remark 5 As L_0 in Lemma 2 is sufficiently large, the upper bound of the convergence rate η in (2.43) would decrease as the condition number of M increases.

Proof Suppose the minimal and maximal eigenvalues of M are $\underline{\lambda}_M$ and $\bar{\lambda}_M$. We can see that the convergence rate is related to c, C and D from (2.43). Firstly, we see that c is not related to M for large L_0 , since $\frac{c_1}{1-\alpha} \geq \frac{\alpha}{(4\alpha-2)\underline{\lambda}_M}$ by (2.25), (2.26) and $M \geq L_0 \mathbf{I}$ when L_0 is large enough. Note that here c is related to c_2 in (2.26). Furthermore, we can choose $D = \underline{\lambda}_M D_0$ from (2.37) and $C = \sqrt{\bar{\lambda}_M} C_0$ from (2.36) and the fact $\bar{\lambda}_M \|x\|^2 \geq \|x\|_M^2 \geq \underline{\lambda}_M \|x\|^2$. Since C_0, D_0 is not related to M , we see $C_1 = \frac{c^2 C^2}{D} = \frac{c^2 C_0^2}{D_0} \frac{\bar{\lambda}_M}{\underline{\lambda}_M}$ would increase when the condition number of M increases. Thus the upper bound of the convergence rate $\sqrt{1 - \frac{2}{2C_1+3}}$ is decreased when the condition number of M increases. \square

2.3 Preconditioners and Preconditioned DCA_e

Let's first consider the convex subdifferentials ∂P_2^I or ∂P_2^A by the following lemma for more general case.

Lemma 5 *The subdifferential of the convex function $p(x) := \max(|Kx|^2, \tau)/2$ is as follows*

$$\{K^* \chi_{K,\tau}^s Kx \mid s \in [0, 1]\} = \partial_x \left(\frac{1}{2} \max(|Kx|^2, \tau) \right), \quad (2.44)$$

where the constant $\tau > 0$ and $\chi_{K,\tau}^s$ is the generalized Clarke derivatives of $\max(\cdot, 1.0)$,

$$\chi_{K,\tau}^s = \begin{cases} 1, & |Kx|/\sqrt{\tau} > 1.0, \\ s, & |Kx|/\sqrt{\tau} = 1.0, \quad s \in [0, 1], \\ 0, & |Kx|/\sqrt{\tau} < 1.0. \end{cases} \quad (2.45)$$

Furthermore, we have

$$\partial \left(\sum_{i=1}^l \frac{\mu_i}{2} \max(|K_i x|^2, \tau_i) \right) = \left\{ \sum_{i=1}^l \mu_i K_i^* \chi_{K_i, \tau_i}^{s_i} K_i x : s^i \in [0, 1], \quad i = 1, \dots, l \right\}. \quad (2.46)$$

Henceforth, we choose $s^i \equiv 1, i = 1, \dots, l$ throughout this paper.

Proof We mainly need to consider (2.45). Since for each $p_i(x) := \frac{\mu_i}{2} \max(|K_i x|^2, \tau_i), i = 1, \dots, l$, $\text{dom } p_i = X$ which is the whole domain, then by [34] (Theorem 23.8), we have

$$\partial \left(\sum_{i=1}^l p_i(x) \right) = \sum_{i=1}^l \partial p_i(x).$$

Let's consider the Clarke's generalized subdifferential of $p(x)$. Denote $p_1(x) = \frac{1}{2}|Kx|^2$ and $p_2(x) = 0$. It can be seen that $p(x)$ is a PC^1 function [37]. It can be easily checked that while $|Kx| > \sqrt{\tau}$,

$$\langle \nabla_x \left(\frac{1}{2}|Kx|^2 \right), y \rangle = \langle Kx, Ky \rangle,$$

where the inner product above is understood in the usual vector inner product such as $a^T b$. We thus have $(\nabla_x p_1)(y) = \chi_{K, \tau}^s \langle Kx, Ky \rangle$ with $s = 1$ for $|Kx| > \sqrt{\tau}$. $\nabla_x p_2(x) = 0$ follows easily. We thus conclude that [37] (Proposition 4.3.1)

$$\partial_x p(x) = \text{co}\{\nabla_x p_1(x), \nabla_x p_2(x)\},$$

where the notation "co" denotes the convex hull of the corresponding set [17]. Since for convex functions, the Clarke generalized subdifferential coincides with their convex subdifferential [17] (Proposition 2.2.7), we have (2.44). \square

Now we turn to the preconditioners for image denoising. According to Lemma 2, we call a preconditioner M_p *feasible* for T if and only if

$$M_p \geq T = L_0 \mathbf{I} - \mu \Delta,$$

where L_0 is the same as in Lemma 2. For operators of type $T = \alpha \mathbf{I} - \beta \Delta$ for $\alpha, \beta > 0$ where $\Delta = \text{div } \nabla$ can be interpreted as a discrete Laplace operator with homogeneous Neumann boundary conditions [6, 7]. In other words: solving $Tx = b$ correspond to a discrete version of the boundary value problem

$$\begin{cases} \alpha \mathbf{x} - \beta \Delta \mathbf{x} = b, \\ \frac{\partial \mathbf{x}}{\partial \nu} |_{\partial \Omega} = 0. \end{cases} \quad (2.47)$$

Besides Remark 1, here are some examples from the classical iterative methods for linear systems.

Example 1

- Obviously, $M_p = T$ with $L_0 = L$ is a feasible preconditioner for T in (2.51). This choice reproduces the original proximal DCA with $M = L\mathbf{I}$ without preconditioners.
- The choice $M_p = c\mathbf{I}$ with $c \geq L + \mu \|\nabla\|^2$ also yields a feasible preconditioner. This is corresponding to the Richardson method, where the update for x^{k+1} can be seen as an explicit step.

We employ the efficient symmetric Red-Black Gauss-Seidel (SRBGS) iterations as the preconditioner [6, 7]. Of course, several steps of this preconditioner can also be performed; see the following Proposition 3. Furthermore, we denote the n -fold application of the symmetric Red-Black to the initial guess x and right-hand side b by [6, 7]

$$\text{SRBGS}_{\alpha, \beta}^n(x, b) = (\mathbf{I} + M_p^{-1}(\mathbf{1}_b - T))^n x \quad (2.48)$$

making it again explicit that M_p and T depend on α and β .

Proposition 3 ([6]) *Let M_p be a feasible preconditioner for T and $n \geq 1$. Then, applying the preconditioner n times, i.e.,*

$$\begin{cases} x^{k+(i+1)/n} = x^{k+i/n} + M_p^{-1}(b^k - Tx^{k+i/n}) \\ i = 0, \dots, n-1 \end{cases}$$

corresponds to $x^{k+1} = x^k + M_{p,n}^{-1}(b^k - Tx^k)$ where $M_{p,n}$ is a feasible preconditioner.

It is proved in [6] that $M_{p,n} \geq T$. We thus conclude that the corresponding metric in the proximal term in (2.8) M_n is positive definite, since $M_n = M_{p,n} + \mu\Delta \geq T + \mu\Delta \geq L_0\mathbf{I}$. Proposition 3 provides great flexibility for choosing how many inner preconditioned iterations for the linear subproblems.

Remembering $\nabla x = [\nabla_1 x, \nabla_2 x]^T$ and $|\nabla x|^2 = |\nabla_1 x|^2 + |\nabla_2 x|^2$, let's denote

$$\chi_x = \begin{cases} 1, & |\nabla x| \geq \sqrt{\frac{\lambda}{\mu}}, \\ 0, & |\nabla x| < \sqrt{\frac{\lambda}{\mu}}, \end{cases} \quad \chi_{x,1} = \begin{cases} 1, & |\nabla_1 x| \geq \sqrt{\frac{\lambda}{\mu}}, \\ 0, & |\nabla_1 x| < \sqrt{\frac{\lambda}{\mu}}, \end{cases} \quad \chi_{x,2} = \begin{cases} 1, & |\nabla_2 x| \geq \sqrt{\frac{\lambda}{\mu}}, \\ 0, & |\nabla_2 x| < \sqrt{\frac{\lambda}{\mu}}. \end{cases}$$

With these preparations, we give the following Algorithm 2. For color images, denoting the color

Algorithm 2 preDCA_e for image denoising or segmentation of the truncated model (ITQ) or (ATQ) with $A = \mathbf{I}$

$x^0 \in \text{dom } P_1$, $\{\beta_t\} \subseteq [0, 1)$, with $\sup_t \beta_t < 1$. Choose $L_0 \geq L$ and set $x^{-1} = x^0$.
Iterate the following steps for $t = 0, 1, \dots$,

$$\xi^t = \begin{cases} \nabla^* \chi_{x^t} \nabla x^t, & \text{for the isotropic case,} \\ (\nabla_1^* \chi_{x^t,1} \nabla_1 + \nabla_2^* \chi_{x^t,2} \nabla_2) x^t, & \text{for the anisotropic case,} \end{cases} \quad (2.49)$$

$$y^t = x^t + \beta_t(x^t - x^{t-1}), \quad (2.50)$$

$$b^t = (L_0 - \mathbf{I})y^t + \nabla f|_{y=y^t} + \xi^t, \quad (2.51)$$

$$x^{t+1} = \text{SRBGS}_{\alpha,\beta}^n(y^t, b^t), \quad T := (L_0\mathbf{I} - \mu\Delta).$$

Unless some stopping criterion is satisfied, stop

image as $\mathbf{x} = (\mathbf{x}_1, \mathbf{x}_2, \mathbf{x}_3)^T$, the truncated quadratic regularization models are as follows

$$\arg \min_{\mathbf{x}} \mathcal{F}(\mathbf{x}) = \frac{\|\mathbf{A}\mathbf{x} - \mathbf{x}_0\|_2^2}{2} + \sum_{i=1}^m \sum_{j=1}^n \frac{\mu}{2} \min(|(\nabla \mathbf{x})_{i,j}|^2, \frac{\lambda}{\mu}), \quad \text{isotropic case} \quad (2.52)$$

$$\arg \min_{\mathbf{x}} \mathcal{F}(\mathbf{x}) = \frac{\|\mathbf{A}\mathbf{x} - \mathbf{x}_0\|_2^2}{2} + \sum_{i=1}^m \sum_{j=1}^n \sum_{k=1}^3 \frac{\mu}{2} \min(|(\nabla \mathbf{x}_k)_{i,j}|^2, \frac{\lambda}{\mu}), \quad i = 1, 2, 3, \quad \text{anisotropic case}$$

where $|\nabla \mathbf{x}|^2 = \sum_{i=1}^3 |\nabla \mathbf{x}_i|^2$ and $|\nabla \mathbf{x}_i|^2 = |\nabla_1 \mathbf{x}_i|^2 + |\nabla_2 \mathbf{x}_i|^2$, $i = 1, 2, 3$ and \mathbf{A} is a linear and bounded operator. It can be seen that the functional of the isotropic case in (2.52) is still within the form of Theorem 1. For the anisotropic case, denoting $\mathbf{K}_1 = \text{Diag}[\nabla, 0, 0]$, $\mathbf{K}_2 = \text{Diag}[0, \nabla, 0]$ and $\mathbf{K}_3 = \text{Diag}[0, 0, \nabla]$, then the functional

$$\sum_{i=1}^3 \frac{\mu}{2} \min(|\nabla \mathbf{x}_i|^2, \frac{\lambda}{\mu}) = \sum_{i=1}^3 \frac{\mu}{2} \min(|\mathbf{K}_i \mathbf{x}|^2, \frac{\lambda}{\mu}),$$

is still of the form in Theorem 1 before the summation over all the pixels as in (2.52). The global convergence and local linear convergence rate also follow. The corresponding algorithm is completely similar to Algorithm 2 and we omit here.

3 Numerics

In this section, we will consider the image denoising and image segmentation problem. All experiments are performed in Matlab 2019a on a 64-bit PC with an Inter(R) Core(TM) i5-6300HQ CPU(2.30Hz) and 12 GB of RAM.

3.1 Image Denoising

We will compare with the well-known total variation (TV) regularization

$$\arg \min_{\mathbf{x} \in X} F(\mathbf{x}) = \frac{1}{2} \|\mathbf{A}\mathbf{x} - f\|_2^2 + \alpha \|\nabla \mathbf{x}\|_1, \quad (3.1)$$

For image denoising, $A = \mathbf{I}$. The first-order primal-dual algorithm is employed for the minimization problem (3.1) [12]. We will also compare with the appealing truncated regularization framework developed in [42] including the truncated TV (shorten as TR-TV), truncated logarithmic regularization (shorten as TR-LN), the truncated quadratic regularization (shorten as TR- l_2), and the weighted difference of anisotropic and isotropic total variation mode (Ani-iso-DCA) [26]. The TR- l_2 models are the same as (ITQ) and (ATQ). As in [42], ADMM (Alternating direction method of multipliers) type method is employed to solve the TR-TV, TR- l_2 , and TR-LN. It is already shown TR-TV and TR-LN can give promising PSNR especially for isotropic cases [42]. Here we focus on the anisotropic cases. The extrapolation parameter $\{\beta_t\}$ is chosen according to [39] for the proposed preconditioned DCA, where

$$\beta_t = (\theta_{t-1} - 1)/\theta_t, \quad \theta_t = (1 + \sqrt{4\theta_{t-1}^2 + 1})/2, \quad \theta_{-1} = \theta_0 = 1. \quad (3.2)$$

Restarting strategy is necessary for satisfying the condition $\{\beta_t\} \in [0, 1)$ and $\sup_t \beta_t < 1$. The adaptive β_t in (3.2) can bring out certain acceleration experimentally. With appropriate parameters of λ and β , it can be seen that the truncated regularization (ITQ) and (ATQ) can obtain high quality denoised images; see Figure 2 for the anisotropic truncated quadratic case (ATQ) and Figure 3 for the isotropic truncated quadratic case (ITQ). Especially, there is no staircasing effect for (ITQ) or (ATQ) as the total variation. From Figure 4, it can be seen that the (ATQ) can get better PSNR with less iterations and less computation time compared with the anisotropic TV.

From Table 1 which is focused on the anisotropic cases, it can be seen that both (ATQ) and TR-LN are very competitive with high PSNR values for most cases compared with TV. The TR-TV can get higher SSIM for some cases. Although the same model with the same parameters λ and μ for (ATQ), our proposed preconditioned DCA can get higher PSNR and SSIM compared with ADMM used in [42]. The preconditioned DCA may exploit more potential of the model (ATQ) compared to the ADMM employed in [42]. For the comparison with computational efficiency, Figure 7 tells that while the proposed preconditioned DCA can decrease the energy quickly and achieve a better PSNR value much fast compared with both iteration number and iteration time, the ADMM employed in [42] can obtain a lower energy with enough iterations. Tables 1 also shows that the Ani-iso-DCA [26] is also competitive compared to TV. However, it is not as promising as ATQ and TR-LN models.

For the global convergence with preconditioners, Figure 5 tells that the proposed preconditioned DCA is faster than DCA with solving the linear subproblem very accurately by the DCT (Discrete

cosine transform) compared both with iteration number and computational time. This is surprising that the proposed preconditioned DCA not only can save the computational efforts but also can improve the performance of DCA with more efficient algorithms. For the local convergence rate, Figure 6(a) tells that for the whole nonlinear DCA iterations, for the linear system appeared, the SRBGS preconditioner is very efficient compared to solving the linear subproblems very accurately with DCT. The proposed preconditioned DCA can get faster local linear convergence rate with less computations compared to the original proximal DCA with highly accurate DCT solver. Theoretically, the proposed preconditioned DCA not only provides an efficient inexact framework with any finite time preconditioned iterations for DCA with global convergence guarantee, but also can potentially give a faster local convergence rate compared to the original DCA with a very accurate solver.

Figure 8 shows that the proposed preconditioned DCA can be used for image segmentation with various examples, which is not surprising since the truncated quadratic model is widely studied and used for image segmentation problems [10, 11]. Figure 8 also shows that the truncated quadratic model can give better segmentation than TV.

3.2 Image deblurring

For image deblurring, by Proposition 1, we just need to design a preconditioner for the discrete version of the following equation

$$T_n \mathbf{x} = b^t, \quad T_n := (L_0 \mathbf{I} + A^* A - \mu \Delta_n), \quad \frac{\partial \mathbf{x}}{\partial \nu} = 0, \quad (3.3)$$

where we use Δ_n to denote the Laplacian operator with emphasis on the Neumann boundary condition. The above equation is usually solved directly by FFT (fast fourier transform). However, considering the FFT is based on the periodic boundary condition which does not match the Neumann boundary condition, it can be circumvented through preconditioning technique [7],

$$T_p x = b^t, \quad T_p := (L_0 \mathbf{I} + A^* A - \mu \Delta_p), \quad x \text{ with periodic boundary condition}, \quad (3.4)$$

where Δ_p denotes the Laplacian operator with emphasis on the periodic boundary condition. It is proved that $T_p \geq T_n$ [7]. We can use T_p as a preconditioner for T_n as follows

$$x^{t+1} = y^t + T_p^{-1}(b^t - T_n y^t) = T_p^{-1}(b^t + T_p y^t - T_n y^t) = T_p^{-1}(b^t - \mu(\Delta_p - \Delta_n)y^t).$$

Since $T_p = A^* A - \mu \Delta_n + M$ by Proposition 1, we have the proximal metric $M = T_p - T_n + L_0 \mathbf{I} \geq L_0 \mathbf{I}$. Denoting the periodic convolution kernel of $-\Delta$ is κ_Δ along with \mathcal{F} and \mathcal{F}^{-1} being the discrete Fourier and inverse Fourier transform [7], with these preparations, we now give our Algorithm 3 for image deblurring.

For image deblurring of anisotropic cases, we will compare with TV, i.e., $Au = u * \kappa$ in (3.1) with first-order primal-dual algorithm [12], the TR-TV and TR- l_2 models in [42] with ADMM who can get stable PSNR during iterations. We also compared with the DCA without preconditioning by $x^{t+1} = T_p^{-1}(b^t)$ and we denote it as ATQ-Npre. In ATQ-Npre, the different boundary conditions of T_p and T_n are ignored, and FFT together with inverse FFT is directly applied to the Neumann boundary condition T_n .

Figure 9 tells that we can get high quality deblurred images with (ATQ) with our preconditioned DCA, i.e., Algorithm 3 for degraded images blurred by motion filter or Gaussian filter. Here

Algorithm 3 preDCA_e for image deblurring of the truncated model (ITQ) or (ATQ) with $Ax = x * \kappa$ and $A^*x = x * \kappa'$ with κ being the convolution kernel

$x^0 \in \text{dom } P_1$, $\{\beta_t\} \subseteq [0, 1)$, with $\sup_t \beta_t < 1$. Choose $L_0 > 0$ and set $x^{-1} = x^0$.
Iterate the following steps for $t = 0, 1, \dots$,

$$\xi^t = \begin{cases} \nabla^* \chi_{x^t} \nabla x^t, & \text{for the isotropic case,} \\ (\nabla_1^* \chi_{x^t, 1} \nabla_1 + \nabla_2^* \chi_{x^t, 2} \nabla_2) x^t, & \text{for the anisotropic case,} \end{cases} \quad (3.5)$$

$$y^t = x^t + \beta_t(x^t - x^{t-1}), \quad (3.6)$$

$$b^t = L_0 y^t + x_0 * \kappa' + \xi^t, \quad (3.7)$$

$$x^{t+1} = \mathcal{F}^{-1} \left(\frac{\mathcal{F}(b^t)}{|\mathcal{F}(\kappa)|^2 + \mu \mathcal{F}(\kappa_\Delta) + L_0} \right).$$

Unless some stopping criterion is satisfied, stop

Table 1: Comparison for anisotropic image denoising models. The noisy images are as follows: Lena1, Lena2 with size 512×512 , Monarch1 and Monarch2 with size 768×512 . The usual zero mean Gaussian white noise of variance $\sigma = 0.1$ for Lena1 or Monarch1 and $\sigma = 0.05$ for Lena2 or Monarch2. The parameters for the corresponding models are as follows. For (ATQ), we choose $\mu = 3, \lambda = 0.01$ for $\sigma = 0.1$ cases and $\mu = 1.5, \lambda = 0.005$ for $\sigma = 0.05$ cases. For the anisotropic TV model, the regularization parameter α is chosen as the variance of the noise, i.e., $\alpha = \sigma$. For the truncated regularization, the parameters of TR-TV are $\alpha = 10, \beta = 600, \tau = 0.6$ for $\sigma = 0.1$ cases and $\alpha = 40, \beta = 6000, \tau = 0.2$ for $\sigma = .05$ cases. The parameters of TR- l_2 are $\alpha = 2/3, \beta = 6000, \tau = 0.0577$ for $\sigma = 0.1$ cases and $\alpha = 4/3, \beta = 6000, \tau = 0.0577$ for $\sigma = 0.05$ cases. The parameters of TR-LN are $\alpha = 10, \beta = 600, \tau = 0.5, \theta = 1$ for $\sigma = 0.1$ cases and $\alpha = 40, \beta = 600, \tau = 0.5, \theta = 1$ for $\sigma = 0.05$ cases. The parameters of Ani-iso-DCA are $\mu = 5, \lambda = 0.5$ for $\sigma = 0.1$ cases and $\mu = 15, \lambda = 1$ for $\sigma = 0.05$ cases.

	Lena1		Monarch1		Lena2		Monarch2	
	PSNR	SSIM	PSNR	SSIM	PSNR	SSIM	PSNR	SSIM
ATQ model	29.308	0.784	29.620	0.836	32.380	0.859	33.203	0.898
TV model	29.227	0.800	29.143	0.873	31.850	0.854	32.613	0.919
TR-TV	29.250	0.801	29.169	0.875	32.601	0.854	33.178	0.893
TR- l_2	29.079	0.741	27.851	0.768	31.950	0.832	30.975	0.853
TR-LN	29.285	0.800	29.361	0.873	32.615	0.850	33.223	0.887
Ani-iso-DCA	29.113	0.793	29.227	0.864	32.293	0.859	33.000	0.909

we choose $L_0 = 10^{-10}$ to approximate the original linear system (2.5) of the standard DCA. Table 2 shows that (ATQ) with the proposed algorithm can get competitive PSNR and SSIM. Our preconditioned DCA can still obtain better PSNR or SSIM compared the TR- l_2 by ADMM. Both Table 2 and Figure 6(b) shows that (ATQ) with preconditioned DCA in Algorithm 3 can get better PSNR, SSIM and lower energy compared to the DCA without preconditioning, i.e., ATQ-Npre. The performance of Ani-iso-DCA [26] is similar to the denoising case, which is competitive compared to TV.

We also found that Algorithm 3 with small L_0 can get much better PSNR and SSIM than Algorithm 1 for imaging deblurring where the A^*A is put into the backward step. Since whose PSNR and SSIM are much lower according to our experience, we did not present the corresponding numerical results.

4 Discussion and Conclusions

In this paper, we give a thorough study on the proposed preconditioned DCA with extrapolation. We analysis it through the proximal DCA with metric proximal terms. We show that our framework

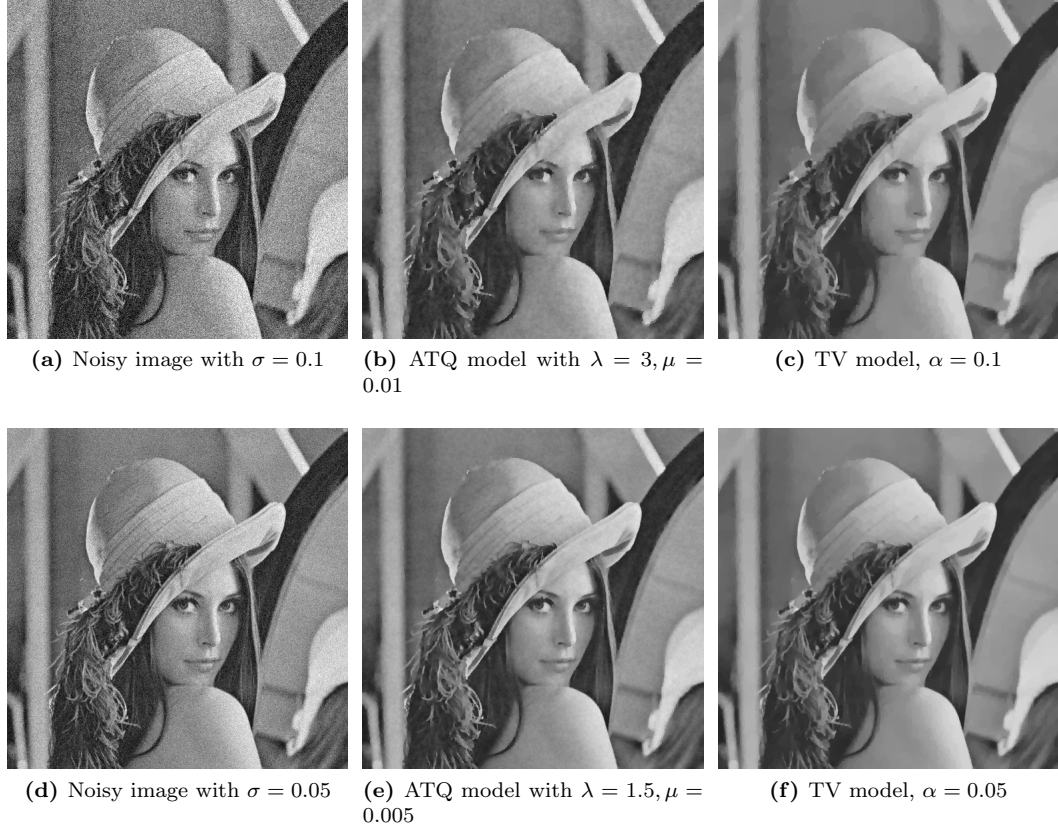


Fig. 2: Images (a) and (d) show the corresponding noisy images of the standard Lena image of size 512×512 corrupted by Gaussian noise of Gaussian variance $\sigma = 0.1$ and $\sigma = 0.05$, i.e., Lena1 and Lena2 image in Table 1. Images (b) and (e) show the denoised images of (a) and (d) with ATQ by parameters $\mu = 3, \lambda = 0.01$ and $\mu = 1.5, \lambda = 0.005$ correspondingly. Images (c) and (f) are denoised images of (a) and (d) by the anisotropic TV through the first-order primal-dual algorithm with the corresponding parameters $\alpha = 0.1$ and $\alpha = 0.05$.

Table 2: Comparison for anisotropic image deblurring models. The first columns are different degraded images. The Kodim251 and Llama1 are both degraded with Gaussian filter with size 11×11 and Gaussian noise of variance $\sigma = .01$. The Kodim252 and Llama2 are both degraded with motion filter with size 40×50 and Gaussian noise of variance $\sigma = .01$. The corresponding parameters are as follows. We choose $\mu = 0.01$ and $\lambda = 10^{-4}$ for both ATQ or ATQ-Npre, $\alpha = 10^{-3}$ for TV, $\alpha = 2000, \beta = 6000, \tau = 0.5$ for TR-TV [42] which turns out better than $\beta = 600$ as in [42], $\alpha = 400, \beta = 500, \tau = 0.1$ for TR- l_2 [42], $\mu = 2, \lambda = 5 \times 10^{-3}$ for Kodim251 and Llama1 cases, and $\mu = 5 \times 10^{-2}, \lambda = 5 \times 10^{-5}$ for Kodim252 and Llama2 cases. The parameters of Ani-iso-DCA are $\mu = 5 \times 10^{-2}, \lambda = 5 \times 10^{-5}$ for Gaussian filter and $\mu = 2, \lambda = 5 \times 10^{-3}$ for motion filter. The Kodiam25 image is taken from <http://www.cs.albany.edu/~xypan/research/snr/Kodak.html>.

	Kodim251		Llama1		Kodim252		Llama2	
	PSNR	SSIM	PSNR	SSIM	PSNR	SSIM	PSNR	SSIM
ATQ model	24.211	0.602	27.771	0.750	23.943	0.603	26.820	0.712
TV model	23.655	0.537	26.960	0.704	23.480	0.537	26.081	0.669
TR-TV	23.959	0.571	27.371	0.728	23.936	0.583	26.643	0.700
TR- l_2	24.112	0.600	27.284	0.707	23.919	0.604	26.450	0.671
ATQ-Npre	24.134	0.599	27.654	0.747	23.835	0.600	26.758	0.710
Ani-iso-DCA	21.832	0.406	24.349	0.562	20.685	0.356	22.962	0.514

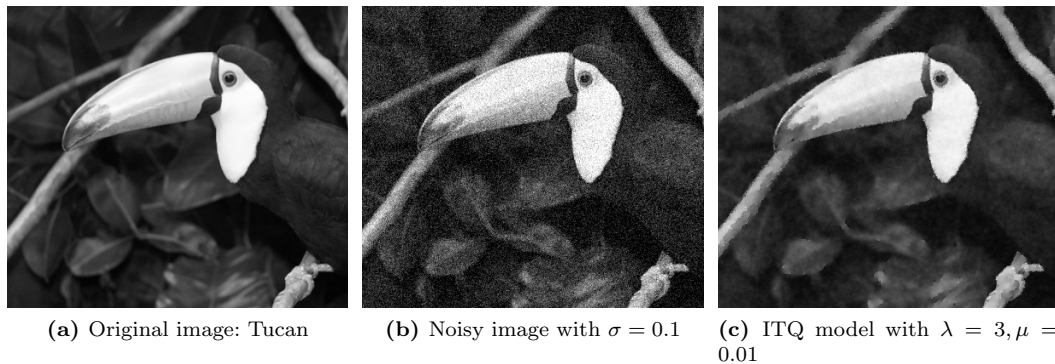


Fig. 3: Images (a) shows the original 400×355 Tucan image. Image (b) is a noisy image corrupted by 10% Gaussian noise. Image (c) shows the denoised image by (ITQ) with parameters $\mu = 3, \lambda = 0.01$.

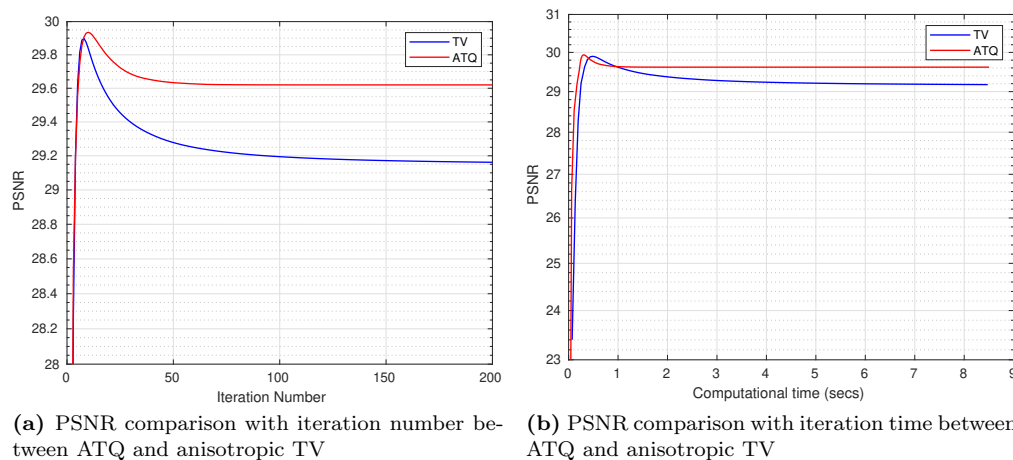


Fig. 4: Figures (a) or (b) shows the PSNR comparisons with iteration number or computational time between (ATQ) and the anisotropic TV. The computations are based on the Monarch image of size 768×512 . The parameters of (ATQ) are $\mu = 3, \lambda = 0.01$ and the parameter of the anisotropic TV is $\alpha = 0.1$.

is very efficient to deal with linear systems, while the global convergence and the local convergence rate can also be obtained. Numerical results show that the proposed preconditioned DCA is very efficient for truncated regularization applying to image denoising and image segmentation. We will consider other challenging tasks or applications with our preconditioned DCA framework.

Acknowledgements H. Sun acknowledges the support of NSF of China under grant No. 11701563. The authors also would like to thank all the anonymous referees for their detailed comments that helped us to improve the manuscript.

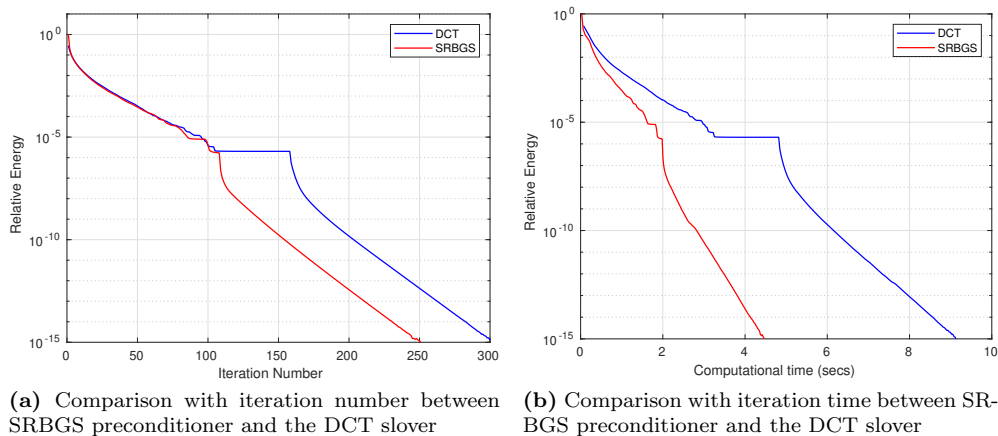


Fig. 5: Figures (a) or (b) shows the comparison with iteration number or computational time between preconditioned DCA with 10 times symmetric Red-Black Gauss-Seidel (SRBGS) iterations and the DCT solver. The DCT solver can be seen as an approximately exact solver without preconditioners, i.e., $M = LI$. The computation is based on Monarch with size 768×512 for the model (ATQ) with parameters $\mu = 3, \lambda = 0.01$.

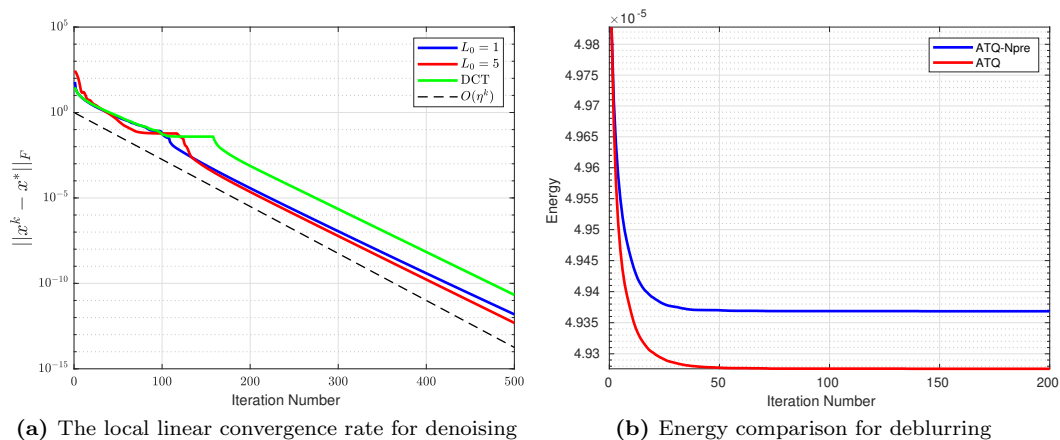
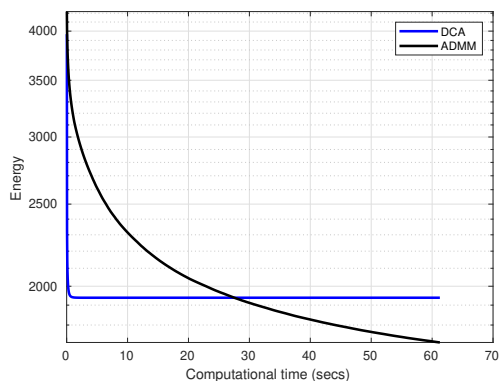


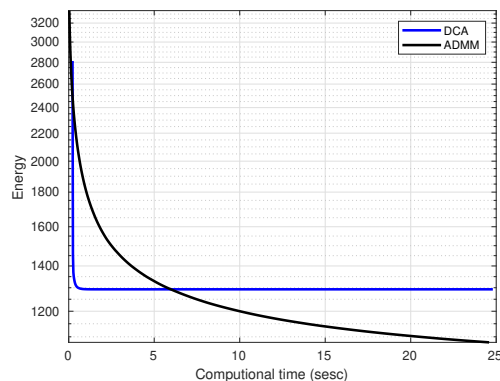
Fig. 6: Figure (a): The local linear convergence rate. The computation is by the model (ATQ) for the Monarch image of size 768×512 with parameters $\mu = 3, \lambda = 0.01$. L_0 is as in Lemma 2 and DCT represents the case $M = LI$ without preconditioner and solving the corresponding linear equation with DCT solver. The preconditioned DCA for different L_0 are both with 10 times symmetric Red-Black Gauss-Seidel (SRBGS) iterations. $\eta \in (0, 1)$ is a constant. Figure (b): The energy of precondition ATQ is lower than that of ATQ without preconditioning (ATQ-Npre) for deblurring the Llamal image with Motion filter blur and parameters $\mu = 0.01, \lambda = 10^{-4}$ as in Table 2.

References

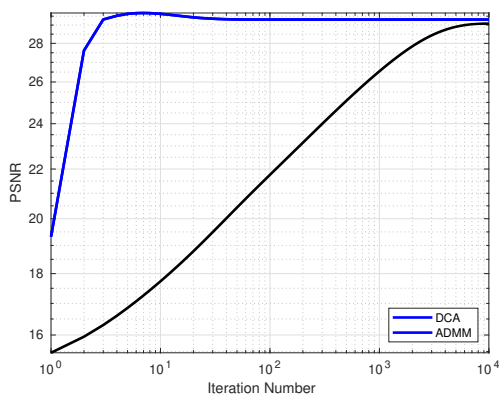
1. H. Attouch, J. Bolte, *On the convergence of the proximal algorithm for nonsmooth functions involving analytic features*, Math. Program., Ser. B, 116, pp. 5–16, 2009, doi:10.1007/s10107-007-0133-5.



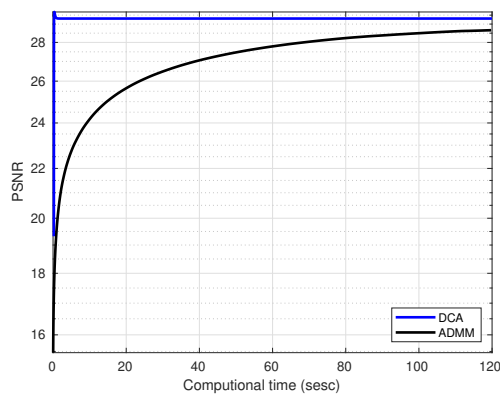
(a) Energy comparison with iteration number between ATQ and anisotropic ADMM



(b) Energy comparison with iteration time between ATQ and anisotropic ADMM



(c) PSNR comparison with iteration number between ATQ and anisotropic ADMM



(d) PSNR comparison with iteration time between ATQ and anisotropic ADMM

Fig. 7: Figures (a) or (b) shows the energy comparisons with iteration number or computational time between (ATQ) and the anisotropic ADMM for image denoising. Figures (c) or (d) shows the PSNR comparison with iteration number or computational time between (ATQ) and the anisotropic ADMM for image denoise. The computations are based on the Lena image of size 512×512 and the zeros mean Gaussian white noise of variance $\sigma = 0.1$ are added to the image. The parameters of (ATQ) are $\mu = 3, \lambda = 0.01$ and the parameters of the anisotropic ADMM is $\alpha = 2/3, \beta = 6000, \tau = 0.0577$.

2. H. Attouch, J. Bolte, P. Redont, A. Soubeyran, *Proximal alternating minimization and projection methods for nonconvex problems: an approach based on the Kurdyka-Lojasiewicz inequality*, Mathematics of Operations Research, 35(2), pp. 438–457, 2010, doi: 10.1287/moor.1100.0449.
3. H. Attouch, J. Bolte, B. F. Svaiter, *Convergence of descent methods for semi-algebraic and tame problems: proximal algorithms, forward-backward splitting, and regularized Gauss-Seidel methods*, Math. Program., 137, pp. 91–129, 2013, doi:10.1007/s10107-011-0484-9.
4. M. Allain, J. Idier, Y. Goussard, *On global and local convergence of half-quadratic algorithms*, IEEE Trans. Image Process., 15, pp. 1130–1142, 2006.
5. G. Aubert, L. Vese, *Variational methods in image restoration*, SIAM J. Numer. Anal., 34(5), pp. 1948–1979, 1997.

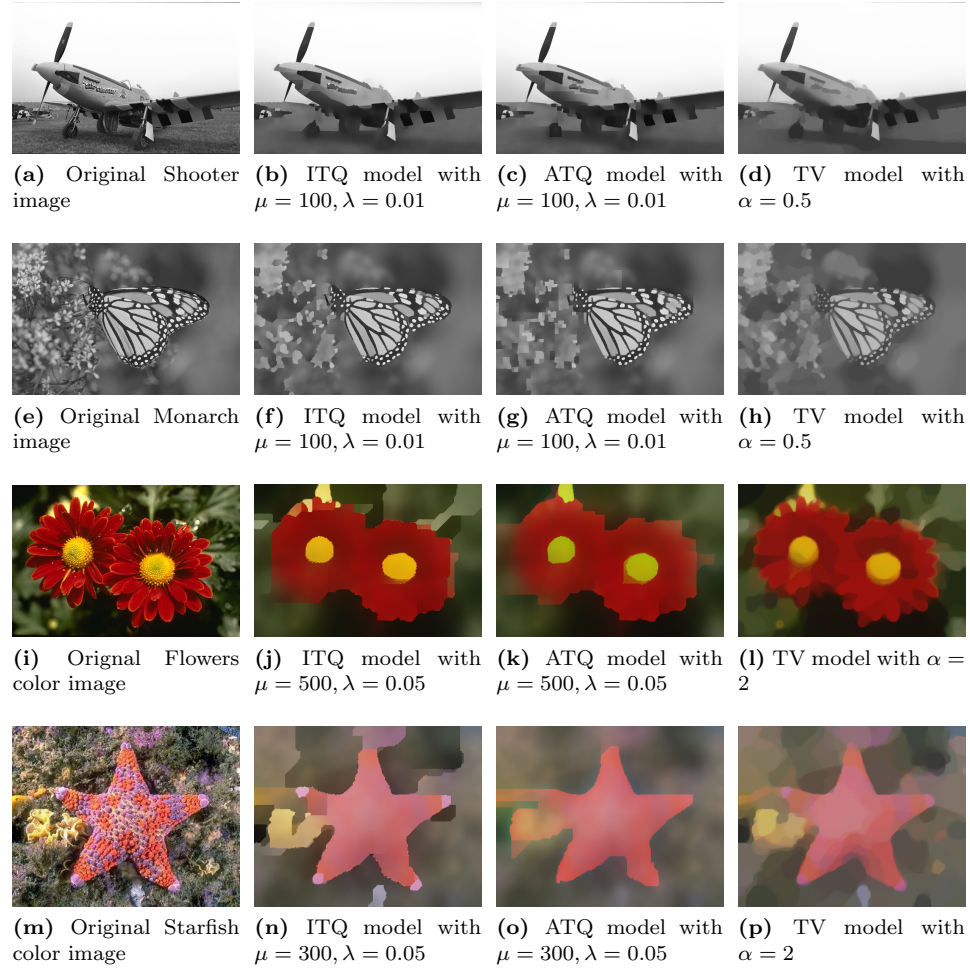


Fig. 8: Images (a), (d), (g), (j) show the original gray image Shooter with size 768×512 , gray image Monarch with size 768×512 , the color image Flowers with size 482×321 , the color image Starfish with size 374×296 respectively. The images in the middle column are segmented by (ITQ) while the images in the right column are segmented by (ATQ). Note that the parameters μ and λ can be different for (ITQ) and (ATQ) even for the same image, since we choose the best parameter as we can find.

6. K. Bredies, H. Sun, *Preconditioned Douglas-Rachford splitting methods for convex-concave saddle-point problems*, SIAM J. Numer. Anal., 53(1), pp. 421–444, 2015.
7. K. Bredies, H. Sun, *Preconditioned Douglas-Rachford algorithms for TV- and TGV-regularized variational imaging problems*, J. Math. Imaging and Vis., 52(3), pp. 317–344, 2015.
8. K. Bredies, H. Sun, *A proximal point analysis of the preconditioned alternating direction method of multipliers*, Journal of Optimization Theory and Applications, 173(3), pp. 878–907, 2017.
9. J. Bolte, S. Sabach, M. Teboulle, *Proximal alternating linearized minimization for nonconvex and nonsmooth problems*, Math. Program., Ser. A, 146, pp. 459–494, 2014, doi: 10.1007/s10107-

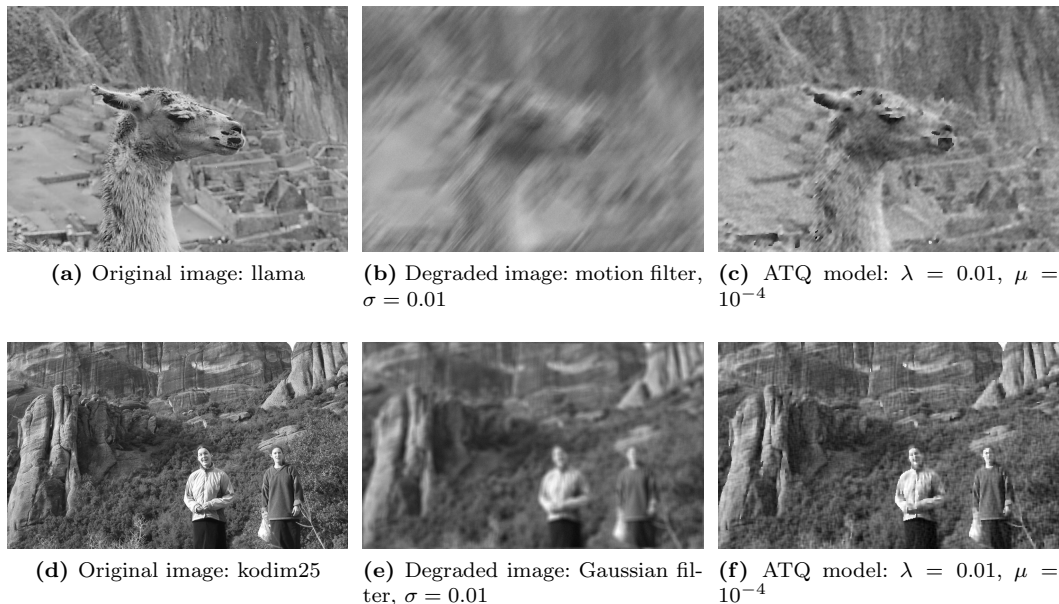


Fig. 9: Images (a) or (d) show the original 513×371 Llama image and 720×436 Kodim25 image. Image (b) is degraded Llama2 image by motion blur as in Table 2. Images (c) shows the reconstructed image by (ATQ) with parameters $\mu = 0.01$, $\lambda = 10^{-4}$. Image (e) is degraded Kodim251 image with Gaussian filter blur as in Table 2. Images (f) shows the reconstructed image by (ATQ) with parameters $\mu = 0.01$, $\lambda = 10^{-4}$.

013-0701-9.

10. Y. Boykov, O. Veksler, R. Zabih, *Fast approximate energy minimization via graph cuts*, IEEE Trans. Pattern Anal. Mach. Intell., 23, pp. 1222–1239, 2001.
11. A. Blake, A. Zisserman, *Visual Reconstruction*, The MIT Press, 1987.
12. A. Chambolle, T. Pock, *A first-order primal-dual algorithm for convex problems with applications to imaging*, J. Math. Imaging and Vis., 40(1), pp. 120–145, 2011.
13. R. Chan, A. Lanza, S. Morigi, F. Sgallari, *Convex non-convex image segmentation*, Numer. Math., 138, pp. 635–680, 2018.
14. A. Chambolle, *Image Segmentation by Variational Methods: Mumford and Shah Functional and the Discrete Approximations*, SIAM J. Appl. Math., 55(3), pp. 827–863, 1995.
15. P. Charbonnier, L. Blanc-Feraud, G. Aubert, M. Barlaud, *Two deterministic half-quadratic regularization algorithms for computed imaging*, Proceedings of 1st International Conference on Image Processing, Austin, TX, vol.2, pp. 168–172, 1994, doi: 10.1109/ICIP.1994.413553.
16. P. Charbonnier, L. Blanc-Feraud, G. Aubert, M. Barlaud, *Deterministic edge-preserving regularization in computed imaging*, IEEE Trans. Image Process., 6, pp. 298–311, 1997.
17. F. H. Clarke, *Optimization and Nonsmooth Analysis*, Vol. 5, Classics in Applied Mathematics, SIAM, Philadelphia, 1990.
18. S. Geman, D. Geman, *Stochastic relaxation, Gibbs distributions, and the Bayesian restoration of images*, IEEE Trans Pattern Anal Mach Intell., PAMI 6, pp. 721–741, 1984.

19. F. R. Hampel, E. M. Ronchetti, P. J. Rousseeuw, W. A. Stahel, *Robust Statistics: The Approach Based on Influence Functions*, John Wiley & Sons, Inc, 1986.
20. D. Geman, C. Yang, *Nonlinear image recovery with half-quadratic regularization*, IEEE Trans. Image Process., 4(7), pp. 932–946, 1995, doi: 10.1109/83.392335.
21. H. A. Le Thi, D. T. Pham, *Difference of convex functions algorithms (DCA) for image restoration via a Markov random field model*, Optimization and Engineering, 18(4), pp. 873–906, 2017, doi: 10.1007/s11081-017-9359-0.
22. H. A. Le Thi, D. T. Pham, *Convex analysis approach to D. C. Programming: theory, algorithms and applications*, Acta Mathematica Vietnamica, 22(1), pp. 289–355, 1997.
23. H. A. Le Thi, D. T. Pham, *DC programming and DCA: thirty years of developments*, Math. Program., Ser. B, 169, pp. 5–68, 2018, doi: <https://doi.org/10.1007/s10107-018-1235-y>.
24. G. Li, TK Pong, *Calculus of the exponent of Kurdyka-Lojasiewicz inequality and its applications to linear convergence of first-order methods*, Found. Comput. Math. 18: pp. 1199–1232, 2018, doi: 10.1007/s10208-017-9366-8.
25. P. Li, W. Chen, H. Ge, and K. M. Ng, l_1 - l_2 minimization methods for signal and image reconstruction with impulsive noise removal, Inverse Problems, 36: 055009, 2020.
26. Y. Lou, T. Zeng, S. Osher, J. Xin, *A weighted difference of anisotropic and isotropic total variation model for image processing*, SIAM J. Imag. Sci., 8, pp. 1798–823, 2015.
27. X.-D. Luo, Z.-Q. Luo, *Extension of Hoffman’s Error Bound to Polynomial Systems*, SIAM Journal on Optimization, 4(2), pp. 383–392. 1994, doi:10.1137/0804021.
28. B. Mordukhovich, *Variational analysis and generalized differentiation I: Basic Theory*, Grundlehren der Mathematischen, Wissenschaften, vol. 330, Springer, Heidelberg, 1998.
29. D. Mumford, A. Desolneux, *Pattern Theory: The Stochastic Analysis of Real-World Signals*, A K Peters, Ltd. Natick, Massachusetts, 2010.
30. D. Mumford, J. Shah, *Boundary detection by minimizing functionals*, I, in Proc. IEEE Conf. on Computer Vision and Pattern Recognition, San Francisco, CA, 1985.
31. D. Mumford, J. Shah, *Optimal approximation by piecewise smooth functions and associated variational problems*, Comm. Pure Appl. Math., 42, pp. 577–684, 1989.
32. M. Nikolova, *Markovian reconstruction using a GNC approach*, IEEE Trans. Image Process., 8(9), pp. 1204–1220, 1999.
33. M. Nikolova, MK. Ng, *Analysis of half-quadratic minimization methods for signal and image recovery*, SIAM J. Sci. Comput., 27(3), pp. 937–966, 2005.
34. R. T. Rockafellar, *Convex Analysis*, Princeton University, 1970.
35. R. T. Rockafellar, R. Wets, *Variational Analysis*. Grundlehren der Mathematischen, Wissenschaften, vol. 317, Springer, Heidelberg, 1998.
36. Y. Saad, *Iterative Methods for Sparse Linear Systems: Second Edition*, Society for Industrial and Applied Mathematics, 2003.
37. S. Scholtes, *Introduction to Piecewise Differentiable Equations*, Springer Briefs in Optimization, Springer, New York, 2012.
38. E. Strekalovskiy, D. Cremers, *Real-time minimization of the piecewise smooth Mumford-Shah functional*, In: Fleet D., Pajdla T., Schiele B., Tuytelaars T. (eds) Computer Vision – ECCV 2014, ECCV 2014, Lecture Notes in Computer Science, vol 8690, Springer, Cham.
39. B. Wen, X. Chen, TK. Pong, *A proximal difference-of-convex algorithm with extrapolation*, Comput. Optim. Appl. 69: pp. 297–324, 2018, doi: 10.1007/s10589-017-9954-1.
40. G. Winkler, *Image Analysis, Random Fields and Markov Chain Monte Carlo Methods : A Mathematical Introduction*, Springer-Verlag Berlin Heidelberg, Second Edition, 2003.

-
41. A. L. Yuille, A. Rangarajan, *The concave-convex procedure*, Neural Comput., 15(4), pp. 915–936, 2003.
 42. C. Wu, Z. Liu, S. Wen, *A general truncated regularization framework for contrast-preserving variational signal and image restoration: Motivation and implementation*, Science China Mathematics, 61(9): pp. 1711–1732, 2018.